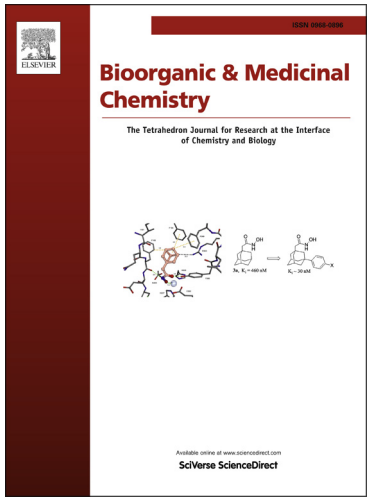

Synthesis and biological evaluation of 2-amino-5-aryl-3-benzylthiopyridine scaffold based potent c-Met inhibitors

Dengyou Zhang, Xiaowei Zhang, Jing Ai, Yun Zhai, Zhongjie Liang, Ying Wang, Yi Chen, Chunpu Li, Fei Zhao, Hualiang Jiang, Meiyu Geng, Cheng Luo, Hong Liu

PII: S0968-0896(13)00653-6
DOI: http://dx.doi.org/10.1016/j.bmc.2013.07.032
Reference: BMC 10996

To appear in: *Bioorganic & Medicinal Chemistry*

Received Date: 1 March 2013
Revised Date: 14 July 2013
Accepted Date: 15 July 2013

Please cite this article as: Zhang, D., Zhang, X., Ai, J., Zhai, Y., Liang, Z., Wang, Y., Chen, Y., Li, C., Zhao, F., Jiang, H., Geng, M., Luo, C., Liu, H., Synthesis and biological evaluation of 2-amino-5-aryl-3-benzylthiopyridine scaffold based potent c-Met inhibitors, *Bioorganic & Medicinal Chemistry* (2013), doi: http://dx.doi.org/10.1016/j.bmc.2013.07.032

Synthesis and biological evaluation of 2-amino-5-aryl-3-benzylthiopyridine scaffold based potent c-Met inhibitors

Dengyou Zhang[a,†], Xiaowei Zhang[b,†] Jing Ai[b,†], Yun Zhai[a], Zhongjie Liang[a], Ying Wang[b], Yi Chen[b], Chunpu Li[a], Fei Zhao[a], Hualiang Jiang[a, c], Meiyu Geng[b,], Cheng Luo[a, *] and Hong Liu[a,*]*

[a] *State Key Laboratory of Drug Research,* CAS Key Laboratory of Receptor Research,*Shanghai Institute of Materia Medica, Shanghai Institutes for Biological Sciences, Chinese Academy of Sciences, 555 Zu Chong Zhi Road, Shanghai 201203, PR China*
[b] *Division of Anti-Tumor Pharmacology, State Key Laboratory of Drug Research, Shanghai Institute of Materia Medica, Chinese Academy of Sciences, Shanghai 201203, PR China*
[c] *School of Pharmacy, East China University of Science and Technology, Shanghai 200237, PR China*
[†] These authors contributed equally to this study.
[*] Correspondence: Hong Liu, Meiyu Geng and Cheng Luo
E-mail: hliu@mail.shcnc.ac.cn or mygeng@mail.shcnc.ac.cn or cluo@mail.shcnc.ac.cn

Keywords:
receptor tyrosine kinase
c-Met
2-amino-5-aryl-3-benzylthiopyridine

A B S T R A C T

A series of 2-amino-*N*-benzylpyridine-3-carboxnamides, 2-amino-*N*-benzylpyridine-3-sulfonamides and 2-amino-3-benzylthiopyridines against c-Met were designed by means of bioisosteric replacement and docking analysis. Optimization of the 2-amino-3-benzylthiopyridine scaffold led to the identification of compound (*R*)-**10b** displaying c-Met inhibition with an IC_{50} up to 7.7 nM. In the cytotoxic evaluation, compound (*R*)-**10b** effectively inhibited the proliferation of c-Met addictive human cancer cell lines (IC_{50} from 0.19 - 0.71 μM) and c-Met activation-mediated cell metastasis. At a dose of 100 mg/Kg, (*R*)-**10b** evidently inhibited tumor growth (45%) in NIH-3T3/TPR-Met xenograft model. Of note, (*R*)-**10b** could overcome c-Met-activation mediated gefitinib-resistance, which indicated its potential use for drug combination. Taken together, 2-amino-3-benzylthiopyridine scaffold was first disclosed and exhibited promising pharmacological profiles against c-Met, which left room for further exploration.

1. Introduction

c-Met, also known as hepatocyte growth factor receptor, is a unique member of receptor tyrosine kinase. *MET* amplification, *MET* mutation, HGF binding or interaction with other membrane receptors could lead to c-Met activation.[1] Aberrant HGF/c-Met signaling has been identified in a wide range of most solid tumors and hematological malignancies.[2,3] Furthermore, c-Met signaling might be responsible for the resistance mechanism in chemotherapy, radiotherapy, other RTK based target therapy and so forth.[4] To date, the main strategies employed to interrupt c-Met signaling pathway involve in blocking the interaction between c-Met and HGF via antibodies[5-16] or antagonists[17-21] and interfering with the active site of the kinase domain with small-molecule kinase inhibitors.[22-47] Among the various strategies, targeting c-Met with small molecules has captured extensive attention, resulting in a respectable number of compounds reaching the clinical stages.[42]

Recently, 2-aminopyridine based c-Met inhibitors have been widely investigated (**Figure 1**).[26,28,43-47] Since researchers at Pfizer reported the 2-amino-3-benzyloxypyridine (**Figure 1**, 2) was an excellent scaffold against c-Met , which culminated in the discovery of crizotinib,[26] pharmaceutical research community was keen to synthesize aminopyridine analogs in pursuit of effective c-Met inhibitors. OSI presented a series of 4,5- or 2,3-fused aminopyridine derivatives[44] (**3**, **4**) with IC_{50} < 0.1 μM. Another interesting modification was the addition of one atom to the amino pyridine core (**5**) reported by Xcovery.[47] Lee et al. also reported a series of c-Met inhibitors with c-Met IC_{50} up to 8 nM in which C-3 position of amino pyridine was substituted with benzoxazole (**6**).[28]

Figure 1

Generally, from the viewpoint of the interaction between small molecules and c-Met protein, these structures feature an aminopyridine core responsible for H-bonding with the hinge region, an aryl fragment extending into the inside pocket and a substituent R facing to the solvent accessible region (**Figure 1**). Furthermore, a flexible *sp3* (**2**, **3**, **5**) or rigid *sp2* (**4**, **6**) functionality as a linker was compatible at the C-3 position of the aminopyridine core. Despite various modifications of the central aminopyridine cores, the aryl fragments and substituents R pursued by medicinal chemists, much less attention was paid to the modification of the linker X between the aminopyridine core and aryl fragment. Therefore, there still remains room for exploration of the new linkers, which might give rise to new generation of aminopyridine based c-Met inhibitors.

Undoubtedly, application of bioisosteres still plays an important role in contemporary drug design, which has often been deployed to improve potency, alter selectivity and address pharmacokinetic issues or to obtain intellectual property. Here, we questioned whether the known *O*-linker (**2**, **3**, **5**)could be simply replaced by other flexible atoms and the rigid linker (**4**, **6**) could be changed into other bioisosteric functionalities. In combination with full consideration of the bio-isosteres and synthetic feasibility, we propose three novel amino pyridine scaffolds with amide (**8**), sulfonamide (**9**) and S-linkers (**10**), respectively (**Figure 1**). Besides, it is reasonable that 2,6-dichloro-3-fluorobenzyl fragment was kept due to its potential π-π interaction with the residue Tyr1230 of c-Met kinase.

Initially, molecular modeling research was performed to ascertain the designed linker. Binding modes of representative compounds (**Table 1**, **8b**, **9b** and **10b**) were compared with a known c-Met inhibitor (crizotinib),[26] as shown in **Figure 2.** The amide linker compound **8b** (**Figure 2A**) keeps the key H-bonding with Met 1160 and Pro1158. The longer bond length of amide than that of oxygen orients the 2,6-dichloro-3-fluorobenzyl fragment forming parallel-displaced rather than face to face π-π interaction (in crizotinib) with Tyr 1230. In addition, the 5-pyrazol-4-yl group goes through a lipophilic tunnel surrounded by Ile 1084 and Tyr 1159. With regard to the sulfur linker, compound **10b** (**Figure 2C**) displayed almost an identical conformation as crizotinib. That the C-S bond is approximately 0.4 Å longer than C-O bond has a little impact on π-π interaction between 2,6-dichloro-3-fluorobenzyl group and Tyr 1230, which may be ascribed to the smaller C-S-C angle fitting the 2,6-dichloro-3-fluorobenzyl group into a right position for π-π stacking. Meanwhile, the aminopyridine core in compound **10b** H-bonds well with the hinge region. While for the sulfonamide linker compound **9b** (**Figure 2B and 2D**), it could adopt two completely different conformations in the active site. One conformation was reasonable and consistent with crizotinib as respected. Yet the other one showed the almost inverted conformation, suggesting that the sulfonamide linker might be incompatible with the inside pocket. Taken together, these observations theoretically indicated that the amide, sulfur and sulfonamide linkers designed here were reasonable and might furnish novel promising c-Met inhibitors.

Figure 2

To test the design idea, a project for the synthesis of these novel aminopyridine scaffolds was launched. The scaffolds of **8** and **9** were readily constructed from corresponding starting materials whereas the preparation of the scaffold of **10** was relatively complicated due to limited synthetic approaches. One indirect method for the construction of **10** has been developed from the known *N*,*N*′-dimethyl-1-[(2-nitropyridin-3-yl)sulfanyl]formamide,[48] which was used as a masked synthon of 2-nitropyridine-3-thiol. Herein, we disclosed our efforts to the synthesis and biological evaluation of these new amino pyridine derivatives.

2. Chemistry

The construction of 2-amino-*N*-benzyl-5-bromopyridine-3-carboxamide core **8a** began with 1-(2,6-dichloro-3-fluorophenyl)ethanone **11**, as presented in **Scheme 1**. Reduction of 2,6-dichloro-3-fluoroacetophenone with $NaBH_4$ afforded benzyl alcohol**,** which was converted to its mesylate **12**. Substitution of **12** with sodium azide, followed by reduction of the resulting benzyl azide with Zn/NH_4Cl,[49] delivered intermediate **13**. Condensation of **13** with 2-amino-5-bromopyridine-3-carboxylic acid smoothly furnished **8a**.

Scheme 1

The chlorosulfonation[50] of 2-amino-5-bromo pyridine afforded 2-amino-5-bromopyridine-3-sulfonyl chloride **15**, which was immediately used for coupling with benzyl amine **13** to give 2-amino-*N*-benzyl-5-bromopyridine-3-sulfonamide core **9a** (**Scheme 2**).

Scheme 2

As shown in **Scheme 3**, compared with **8a** and **9a**, the synthesis of 3-(benzylsulfanyl)-5-bromopyridin-2-amine core **10a** was not straightfoward. Initially, we aimed to obtain 2-nitropyridine-3-thiol by hydrolysis of the known intermediate **18**.[48] Unfortunately, attempt to purify the 2-nitropyridine-3-thiol on silica gel column proved unsuccessful due to its oxidative

dimerization. Therefore, we attempted to perform the reaction in one-pot sequential fashion in order to take advantage of the thiol anion in situ**.** After extensive attempts, the intermediate **20** was readily prepared from **18** through sequential hydrolysis of the dimethylcarbamothioate, trapping of the thiol anion by benzyl methanesulfonate **12** and reduction of the nitro group. Next, bromination of **20** smoothly furnished **10a**.

Scheme 3

With the key intermediate **8a**, **9a** and **10a** in hand, we set out to derivatize the bromide on the C-5 position by employing the pyrazole fragments, since they were frequently used to modulate the chemical properties and biological activity of amino pyridine based c-Met inhibitors.[42] First, a series of pyrazolyl-4-boronic esters were synthesized as depicted in **Scheme 4**. Alkylation of 4-bromo-1*H*-pyrazole, followed by Miyaura boration, delivered boronic esters **25b-e**. Acylation of commercial available **23b** proceeded well to afford **25a**.

Scheme 4

Next, introduction of the pyrazole fragments at the C-5 position of **8a**, **9a** and **10a** was readily achieved by Suzuki coupling (**Scheme 5**). Further derivatization of the N-1 position of the pyrazole was also conducted. The intermediate **31** was converted to its corresponding amide **10g** through hydrolysis of the ester, followed by condensation of the resulting acid with dimethylamine hydrochloride. The deprotection of the Boc groups of 2**8-30** smoothly gave compounds **8b**, **9b** and **10b**. **10b** was subsequently transformed to compounds **10h-j**.

Scheme 5

To gain insight into SAR at C-5 position of **10a**, other heteroaryl and aryl fragments were introduced through Suzuki coupling of the intermediate **10a** with corresponding boronic esters (**10k-10o**). Compounds **36a-l** were prepared in a similar manner as described for compound **10g** in **Scheme 6**.

Scheme 6

The chiral synthesis of (*R*)-**10b** was depicted in **Scheme 7**. Reduction of the ketone **11** furnished the racemic alcohol intermediate **37**. Chemical resolution of **37** afforded the (*S*)-alcohol **38** by use of the Boc protected proline. Then the (*R*)-**10a** intermediate was smoothly obtained in a similar manner as described for **10a** in **Scheme 3**. Suzuki coupling of (*R*)-**10a** with the boronic ester **25d**, followed by the removal of the Boc protective group, gave the desired compound (*R*)-**10b**.

Scheme 7

3. Biology

3.1. ELISA kinase assay.

kinase activity was evaluated according to the enzyme-linked-immunosorbent assay. Briefly, 20 μg/mL poly $(Glu,Tyr)_{4:1}$ (Sigma) was pre-coated as a substrate in 96-well plates. 50 μL of 10 μmol/L ATP solution diluted in kinase reaction buffer (50 mmol/L HEPES pH 7.4, 50 mmol/L $MgCl_2$, 0.5 mmol/L $MnCl_2$, 0.2 mmol/L Na_3VO_4, 1mmol/L DTT) was added to each well. 1μL of various concentrations of indicated compounds diluted in 1% DMSO (v/v) (Sigma) were added to each reaction well. 1% DMSO (v/v) was used as negative control. The kinase reaction initiated after the addition of purified tyrosine kinase proteins diluted in 49 μL of kinase reaction buffer solution. After incubation for 60 min at 37°C, the plate was washed three times with Phosphate Buffered Saline (PBS) containing 0.1% Tween 20 (T-PBS). 100 μL anti-phosphotyrosine (PY99) antibody (1:1000 diluted in 5 mg/mL BSA T-PBS) was then added. After 30 min incubation at 37°C, the plate was washed three times. 100 μL horseradish peroxidase-conjugated goat anti-mouse IgG (1:2000 diluted in 5 mg/mL BSA T-PBS) was added. The plate was then incubated at 37°C for 30 min, and washed 3 times. 100 μL of a solution containing 0.03% H_2O_2 and 2 mg/ml o-phenylenediamine in 0.1 mol/L citrate buffer, pH 5.5, was added. The reaction was terminated by the addition of 50 μL of 2 mol/L H_2SO_4 as color changed, and the plate was read using a multi-well spectrophotometer (SpectraMAX 190, Molecular Devices) at 490 nm. The inhibition rate (%) was calculated using the following equation: [1-(A490/A490 control)] x 100%. IC_{50} values were calculated from the inhibition curves. For ATP competition assay, various concentrations of ATP were diluted for the kinase reaction. TheLineweaver-Burke plot was drawn by Prism.

3.2. Cell proliferation assay.

Cells were seeded in 96-well tissue culture plates. On the next day, cells were exposed to various concentrations of compounds and further cultured for 72h. Finally, cell proliferation was determined by using sulforhodamineB (SRB; Sigma) or CCK-8kit (Dojindo).

3.3. Western blot analysis.

Cells were cultured under regular growth conditions to exponential growth phase. Then the cells were treatment with indicated concentration of compound for 2h at 37°C and lysed in 1×SDS sample buffer. Those cell lysates were subsequently resolved on 10% SDS-PAGE, and transferred to nitrocellulose membranes. Membranes were probed with, phospho c-Met and c-Met, phospho-EGFR and EGFR, phospho-ERK1/2 and ERK1/2, phospho-AKT and AKT (All from Cell Signaling Technology) antibodies then subsequently with HRP-conjugated anti-rabbitIgG. Immunoreactive proteins were detected using ECL Plus (GE Healthcare) and images were pictured by ImageQuant LAS 4010 (GE Healthcare).

3.4. Cell cycle analysis.

Cells were treated with compounds at indicated concentration for 24hrs, typsinized and fixed1h at -20°C by 70% ethanol. Then, the fixed cells were stained with propidium iodide (10 μg/mL)for 30 minutes at 37 and cell cycle variables analyzed by fluorescence-activated cell sorting analysis (BD).

3.5. Wounding Heal Assay.

MDCK cells were planted into the wells of 12-well plates and cultured 24-48 h until a uniform monolayer formed. All wounding assays were performed in a serum-free medium by first pre-incubating the cells in the serum-free medium for 30 min before the start of the experiments. A micropipette was used to create a wound in the monolayer by scraping. After washing to remove the detached cells, compounds at indicated concentration were added. Subsequently, the cells were incubated with and without 50 ng/mL recombinant human HGF and placed in a cell incubator (37°C). They were then image captured at 0 and 10h after incubation using phase-contrast microscope.

3.6. MDCK Scattering Assay.

MDCK cells were plated into 96-well plate at a density of 1,500 cells per well. After 24hrs incubation, MDCK cells formed clusters; then, they were cultured with compounds and 50 ng/mL recombinant human HGF in FBS-free medium for another 24hrs.Cells were fixed by 4% paraformaldehyde for 15min at room temperature, and then stained by 0.2% violet purple, washed with water, and allowed to dry before taking photos. Pictures were taken under microscope.

3.7. *In vivo* Antitumor Activity Assay.

Animal experiments were performed according to institutional ethical guidelines of animal care. Well-developed tumors were cut into 1-mm^3 fragments and transplanted s.c. into the right flank of nude mice using a trocar. When the tumor volume reached 100 to 150 mm^3, the mice were randomly assigned into control and treatment groups. Control groups were given vehicle alone, and treatment groups received (*R*)-**10b** or crizotinib as indicated doses via oral administration 7 days per week for 2 weeks. The sizes of the tumors were measured twice per week using microcaliper. The tumor volume (TV) was calculated as: $TV = (\text{length} \times \text{width}^2)/2$, and the relative tumor volume (RTV) was calculated as: $RTV = V_t/V_0$, where V_t is the tumor volume on the day measured and V_0 is the tumor volume on the first day of treatment. Relative tumor volume was shown on indicated days as the median relative tumor volume±SE indicated for groups of mice. T/C values were calculated on the final day of study for drug-treated compared with vehicle-treated mice as $(RTV_{Treated}/RTV_{Control}) \times 100\%$. Significant differences between the treated versus the control groups ($P \leq 0.05$) were determined using Student's t-test.

4. Results and discussion

4.1 Identification and optimization of the 2-amino-3-benzylthiopyridine scaffold

As these novel amino pyridine derivatives against c-Met have not been previously synthesized and evaluated, the initial goal was to identify the optimal linker. The c-Met enzymatic activities of **8b-d**, **9b** and **10b-10j** were summarized in **Table 1**. To our delight, compound **10b** exhibited c-Met inhibition with an IC_{50} of 16.4 nM, whereas compound **8b** was nearly 20-fold less active and compound **9b** displayed no activity at 10 μM. Obviously, these data suggested that sulfur linker (one atom) was more robust than amide and sulfonamide linkers (two atoms). The encouraging results prompted us to investigate SAR about substituents on the pyrazole whilst keeping the sulfur as linker. It was observed that the incorporation of sulfonyl (**10h**) and carbonyl (**10i-j**) on piperidine of **10b** resulted in a remarkable decrease in potency which indicated the basicity of piperidine might be an important factor for c-Met inhibition. Appending non-basic substituents at the *N*-1 position of the pyrazole (**10c-e** and **10g**) was well tolerated, albeit less active than analog **10b**. However, introduction of an

electron-withdraw group (**10f**) was not beneficial for the potency presumably due to the significant change of electron density of the pyrazole.

Table 1

Subsequently, we extended our attention to explore SAR about other aryl/heteroaryl derivatives at the C-5 position of the 3-(benzylthio)pyridin-2-amine scaffold. The result was shown in **Table 2**. Introduction of the "naked" pyrimidine (**10k**) displayed moderate c-Met inhibition at 0.15 μM. The pyridinyl analogs **10l** and **10m** with the incorporation of polar fragments were more effective and the IC_{50} reached to 26.5 nM and 66.2 nM respectively. Among the phenyl derivatives (**10n-o** and **36a**), benzamide analog **36a** demonstrated potent c-Met inhibition with an IC_{50} of 25.8 nM. At this juncture, it seemed that various aryl/heteroaryl substituents such as phenyl, pyrazoyl and pyridinyl were compatible at the C-5 position.

Table 2

Given the promising enzymatic activity and easy derivation, benzamide analogs at the C-5 postion were prepared for more in-depth SAR exploration (**Table 3**). The simple change of the 1-methylpiperazine to morpholine (**36b**) or dimethyl amine (**36c**) caused nearly 2-fold loss of activity. Introduction of the isopropyl, methylsulfonyl or hydroxyethyl group on the piperazine also proved to be inefficient (**36d-f**). Replacement of the 1-methylpiperazine with the 4-(pyrrolidin-1-yl)piperidine (**36g**) retained the potency at 22.1 nM. The *N*-mono substituted amide analog **36h** showed an IC_{50} of 101 nM, suggesting *N,N*•-disubstituents were preferred here. Bearing a fluoride atom adjacent to amide (**36i-36l**) eroded the c-Met inhibition.

Table 3

Subsequently, the preliminary effects of 2-amino-3-benzylthiopyridine derivatives were evaluated on c-Met phosphorylation and c-Met dependent proliferation in MKN and NIH3T3-TPR-Met cell lines (data not shown). The inhibitory effect of compound **10b** was clearly preferred over than other analogs. Therefore, compound **10b** was chosen for the further evaluation. In addition to consideration of configuration affecting the c-Met activity, the two enantiomers of compound **10b** were prepared. Apparently, the *R* enantiomer of **10b** (for *R*, IC_{50} = 7.7 nM, for *S*, IC_{50} = 171.4 nM) was more potent. Therefore, the (*R*)-**10b** was chosen for further evaluation.

4.2 Kinase Selectivity of (*R*)-**10b**

The selectivity of (*R*)-**10b** against tyrosine kinase activity was assessed by screening against c-Met family member, Ron, along with other 15 tyrosine kinases. In contrast to its high potency against c-Met (IC_{50} = 7.7 nM), (*R*)-**10b** showed more than 40-fold less potency against RON, Axl, ALK, and barely inhibited kinase activity against the other 13 tested tyrosine kinases (IC_{50} > 1 μM)(**Table 4**). All these suggested that (*R*)-**10b** is a relatively selective inhibitor of c-Met.

Table 4

4.3 (*R*)-**10b is an ATP Competitive Inhibitor of Met**

To examine whether (*R*)-**10b** acts as an ATP competitive inhibitor, we evaluated the inhibitory potency of (*R*)-**10b** on kinase enzymatic activities using competitive inhibitory assay by introduction of different concentrations of ATP. As shown in **Figure 3**, Lineweaver-Burk plot for inhibition of Met tyrosine kinase by (*R*)-**10b** with respect to ATP concentration showed all curves intersecting the y-intercept at zero, which indicates a competitive mechanism of inhibition.

Figure 3

4.4 (*R*)-**10b Inhibits c-Met Phosphorylation and its Downstream Signaling Pathways**

Furthermore, we investigated c-Met-targeting activity of (*R*)-**10b** *in vitro* and *in vivo*. Both natural (MKN-45, SNU-5 human gastric carcinoma cells and EBC-1 NSCLC cells that express elevated levels of constitutively active c-Met) and genetical-modified (NIH-3T3/TPR-Met cells and BaF3/TPR-Met cells that stably express a constitutively active, ligand-independent, oncogenic form of c-Met) c-Met expressing cell lines were selected. We found that (*R*)-**10b** inhibited c-Met phosphorylation in a dose-dependent manner in all these cell lines (**Figure 4**). Furthermore, p44/42 and AKT, the key downstream molecules of c-Met signaling were also inhibited upon treatment with (*R*)-**10b**, which support that (*R*)-**10b** inhibits not only the c-Met activity, but subsequent c-Met downstream signaling as well.

Figure 4

4.5 (*R*)-**10b Inhibits the Proliferation of Met-Addicted Human Cancer Cells**

Further an extended panel of human cancer cell lines with different settings of c-Met expression/ activation was chosen to test the anti-proliferation effect of (*R*)-**10b**. As shown in **Table 5**, (*R*)-**10b** effectively inhibited the proliferation of human cancer cell lines, however, the IC_{50} values varied widely among these cancer cells. Notably, (*R*)-**10b** showed IC_{50} values of 0.29 ± 0.05, 0.19 ± 0.02, and 0.71 ± 0.16 μM, respectively in c-Met addictive cancer cell lines MKN45, SNU-5 and EBC-1. In contrast, (*R*)-**10b** exerted much less anti-proliferative effects with IC_{50} values around 10-20 μM in low c-Met-expressed and activated cell lines such as MDA-MB-231, MCF-7 and NCI-H661. Moreover, (*R*)-**10b** significantly inhibited proliferation of NIH-3T3/TPR-Met cells and BaF3/TPR-Met cells, with IC_{50} values of 0.61 ± 0.16 μM and 0.58 ± 0.15 μM, respectively.

Table 5

4.6 (*R*)-**10b Induces G1-phase Cell Cycle Arrest in MKN-45 and Ba/F3-TPR-Met Cells**

To investigate the mechanisms associated with (*R*)-**10b**'s anti-proliferative activity, we explored the effects of (*R*)-**10b** on the cell cycle distribution in MKN-45 cell and Ba/F3-TPR-Met cell. After cells were treated with vehicle or various concentrations of (*R*)-**10b** for 24 h, DNA content in control group displayed a typical histogram observed in exponentially growing cells, while increasing concentration of (*R*)-**10b** arrested cells in G1 phase, with 60.1% of cell population in G1 phase in the presence of 1 μM (*R*)-**10b** in MKN-45 cells (39.1% in control group) (**Figure 5A**). Consistently, (*R*)-**10b** induced G1-phase cell cycle arrest, with 69.6% of cell population in G1 phase in the presence of 1 μM (*R*)-**10b** in BaF3/TPR-Met cells (26.6% in control group) (**Figure 5B**). All these indicated that cell cycle arrest contributed to the anti-proliferative effects of (*R*)-**10b**.

Figure 5

4.7 (*R*)-**10b Inhibits HGF-induced MDCK Cell Scattering and Cell Migration**

It's well known that HGF/c-Met axis promotes cell scattering, a hallmark of cancer invasiveness and metastasis. It is well documented that MDCK cells, which normally grow in clusters, exhibit disruption and scattering of cell colonies on HGF treatment. To determine the effect of (*R*)-**10b** on cell scattering behavior, MDCK cells were treated with HGF in the presence or absence of the agent. As shown in **Figure 6A**, MDCK cells treated with (*R*)-**10b** exhibited inhibitory effect on HGF-induced cell scattering in a dose-dependent manner. At the dose of 3μM, this compound almost completely prevented cell spreading, as evidence by the fact that MDCK cells remain in tight clusters. The enhanced cell migratory ability is involved in the cell scattering phenotype. To examine the effect of (*R*)-**10b** on cell motility, MDCK cells were treated with HGF in the presence of (*R*)-**10b**, and the migration was determined in vitro by a wound-healing assay. As shown in **Figure 6B**, (*R*)-**10b** strongly suppressed HGF-induced cell motility. These results indicated that (*R*)-**10b** strongly inhibited c-Met activation-mediated cell metastasis.

Figure 6

4.8 (*R*)-**10b Overcomes Drug Resistance in Gefitinib-Resistant Cell Line HCC827/GR5**

Since *MET* amplification was previously shown to cause EGFR TKI acquired resistance,[51] we further investigated whether (*R*)-**10b** could overcome EGFR TKI resistance mediated by increased Met signaling. An EGFR TKI gefitinib resistant cell line HCC827/GR5, which derives from a gefitinib sensitive cell line HCC827 and gets acquired resistance due to *MET* amplification was chosen. As expected, the combination of (*R*)-**10b** and gefitinib substantial inhibited the growth of HCC827/GR5 cells, whereas neither agent alone led to growth inhibition (**Figure 7A**).Moreover, in the resistant cells, gefitinib or (*R*)-**10b** effectively reduced EGFR phosphorylation or c-Met phosphorylation, and they had no effects on AKT and p44/42 phosphorylation. (*R*)-**10b** in combination with gefitnib fully suppressed the phosphorylation of AKT and p44/42 (**Figure 7B**). These results indicated that (*R*)-**10b** could overcome c-Met-activation mediated gefitinib-resistance, which implies its potential use for drug combination.

Figure 7

4.9 (*R*)-**10b Inhibits Tumor Growth *in vivo***

To evaluate the Met-inhibitory efficacy of (*R*)-**10b** in animal model, anti-tumor activity of the compound was investigated in the NIH-3T3/TPR-Met xenograft model. In this model, tumor growth is specifically driven by constitutive c-Met activation. We found that oral administration of (*R*)-**10b** at indicated doses for 14 days evidently inhibited tumor growth (tumor growth inhibition of 100 mg/kg was 45.5%) (**Figure 8**). In addition, (*R*)-**10b** was well tolerated, as evidenced by no significant loss of mice body weight after treatment (data not shown).

Figure 8

4.10 Pharmacokinnetic (PK) Profile of (*R*)-10b

The PK profile of compound (*R*)-**10b** was evaluated in rat after single iv (2 mg/kg) and po (10 mg/kg) administration. This compound displayed a half-life time of 5.7 h and a poor oral bioavailability (F = 12.8%), which was attributed to its high clearance (53 mL/min/Kg) and volume of distribution (20 L/Kg). This unfavorable PK profile of (*R*)-**10b** might account for its moderate inhibition of tumor growth.

5. Conclusions

On the basis of reported aminopyridine c-Met inhibitors, a series of 2-amino-*N*-benzylpyridine-3-carboxnamides, 2-amino-*N*-benzylpyridine-3-sulfonamides and 2-amino-3-benzylthiopyridines were designed by means of bioisosteric replacement and docking analysis. We successfully prepared these novel aminopyridine scaffolds. Of particular note, deployment of *N*,*N'*-dimethyl-1-[(2-nitropyridin-3-yl)sulfanyl]formamide as a masked synthon of 2-nitropyridine-3-thiol is the key to construction of 2-amino-3-benzylthiopyridine derivatives.

Initial c-Met enzymatic assay found 2-amino-3-benzylthiopyridines were more robust than 2-amino-*N*-benzylpyridine-3-carboxnamides and 2-amino-*N*-benzylpyridine-3-sulfonamides. Subsequent optimization gave rise to a racemic compound **10b** with potent c-Met enzymatic IC_{50} at 16.4 nM. Further evaluation revealed its *R* configuration compound (*R*)-**10b** displayed c-Met inhibition with an IC_{50} up to 7.7 nM. (*R*)-**10b** was demonstrated to act as an ATP competitive inhibitor. (*R*)-**10b** exhibited dose-dependent inhibition on c-Met phosphorylation and corresponding downstream signaling pathways as well. In the cytotoxic evaluation, compound (*R*)-**10b** effectively inhibited the proliferation a panel of human cancer cell lines such as MKN45, SNU-5 and EBC-1cell lines. (*R*)-**10b** also demonstrated inhibition of c-Met activation mediated cell metastasis. It was worth mentioning that (*R*)-**10b** could overcome c-Met-activation mediated gefitinib-resistance, which implies its potential use for drug combination. At dose of 100 mg/Kg, (*R*)-**10b** evidently inhibited tumor growth (45%) in NIH-3T3/TPR-Met xenograft model.

Although aminopyridine based c-Met inhibitors have been widely investigated, the scaffolds of 2-amino-*N*-benzylpyridine-3-carboxnamide, 2-amino-*N*-benzylpyridine-3-sulfonamide and 2-amino-3-benzylthiopyridine against c-Met were first prepared and biologically evaluated. Among these, 2-amino-3-benzylthiopyridine scaffold exhibited promising pharmacological profiles, which warrant further exploration.

6. Experimental

Unless otherwise noted, the reagents (chemicals) were purchased from commercial sources, and used without further purification. Analytical thin layer chromatography (TLC) was performed on HSGF 254 (0.15-0.2 mm thickness). Compound spots were visualized by UV light (254 nm). Column chromatography was performed on silica gel FCP 200-300 or preparative HPLC (Agilent 1200 series HPLC system, ZORBAX Eclipse XDB-C18, 9.4 × 250 mm, 5 μm). Mircrowave reactions were carried on CEM reactor. NMR spectra were run on 300 or 400 MHz instrument. Chemical shifts were reported in parts per million (ppm, δ) downfield from tetramethylsilane. Proton coupling patterns are described as singlet (s), doublet (d), triplet (t), quartet (q), multiplet (m), and broad (br). Low- and high-resolution mass spectra (LRMS and HRMS) were measured on spectrometer. HPLC analysis of all compounds listed in Tables 1-3 was carried out on an Agilent 1100 Series HPLC with an Agilent Zorbax Eclipse XDB-C18 (4.6 mm × 150 mm, 5 μm) reversed phase column with two solvent systems (MeOH/H_2O and MeOH/H_2O/NH_4OAc). All the assayed compounds displayed a purity of 95-99 % in both solvent systems.

6.1. 1-(2,6-Dichloro-3-fluorophenyl)ethyl methanesulfonate (12).

To a solution of 1-(2,6-dichloro-3-fluorophenyl)ethan-1-one **11** (20.00 g, 96.60 mmol) in 100 mL of MeOH was added portionwise $NaBH_4$ (7.31 g, 193.21 mmol). The resulting mixture was stirred at room temperature for 2h and then quenched with 20 ml of water. After the removal of MeOH under vacuum, the residue was extracted with EA and washed with brine. The organic layer was dried over anhydrous Na_2SO_4 and concentrated under vacuum to afford 1-(2,6-dichloro-3-fluorophenyl)ethan-1-ol, which was pure enough for use in the next step. ^{1}H NMR (400 MHz, $CDCl_3$) δ 7.26 (dd, *J* = 4.8, 8.8 Hz, 1H), 7.02 (dd, *J* = 8.0, 8.8 Hz, 1H), 5.57 (q, *J* = 6.8 Hz, 1H), 2.86 (br, 1H), 1.64 (d, *J* = 6.8 Hz, 3H).

To a solution of 1-(2,6-dichloro-3-fluorophenyl)ethan-1-ol (19.00 g, 90.89 mmol) in 150 ml of CH_2Cl_2 was added Et_3N (13.27 mL, 95.43 mmol) and catalytic amount of DMAP. The resulting solution was cooled in an ice bath and added dropwise MsCl (7.39 mL, 95.43 mmol). After complete addition of MsCl, the reaction mixture was maintained in the ice bath for 1 h and then 30 ml of water was added to the reaction mixture. The organic phase was washed with brine, dried over anhydrous Na_2SO_4 and concentrated under vacuum to afford 1-(2,6-dichloro-3-fluorophenyl)ethyl methanesulfonate (**12**), which was pure enough for use in the next step. Yield: 84%; ^{1}H NMR (300 MHz, $CDCl_3$) δ 7.33 (dd, *J* = 4.8, 9.0 Hz, 1H), 7.12 (dd, *J* = 8.1, 9.0 Hz, 1H), 6.45 (q, *J* = 6.9 Hz, 1H), 2.91 (s, 3H), 1.84 (d, *J* = 6.9 Hz, 3H).

6.2. 1-(2,6-Dichloro-3-fluorophenyl)ethan-1-amine (13).

To a solution of 1-(2,6-Dichloro-3-fluorophenyl)ethyl methanesulfonate 19 (500 mg, 1.74 mmol) in 4 mL of DMF was added NaN_3 (226.4 mg, 3.48 mmol). The resulting mixture was stirred at 50 ºC for 1 h and diluted with 20 ml of water. The mixture was extracted with EA (2 × 10 mL). The organic phase was washed with brine, dried over anhydrous Na_2SO_4 and concentrated under vacuum to afford 2-(1-azidoethyl)-1,3-dichloro-4-fluorobenzene, which was pure enough for use in the next step. ^{1}H NMR (400 MHz, $CDCl_3$) δ 7.31 (dd, *J* = 4.8, 8.8 Hz, 1H), 7.08 (dd, *J* = 8.0, 8.8 Hz, 1H), 5.55 (q, *J* = 6.8 Hz, 1H), 1.65 (d, *J* = 6.8 Hz, 3H).

2-(1-Azidoethyl)-1,3-dichloro-4-fluorobenzene (300 mg, 1.28 mmol) was suspended in 4 mL of EtOH/H_2O (v/v, 3/1). To this suspension was added Zn powder (109 mg, 1.67 mmol) and NH_4Cl (171.4 mg, 3.20 mmol). The reaction mixture was heated at 80 ºC for 1 h. Then the reaction mixture was filtered off and concentrated under vacuum. The residue was partitioned between ethyl acetate and water. The organic phase was washed with brine, dried over anhydrous Na_2SO_4 and concentrated under vacuum to afford 1-(2,6-Dichloro-3-fluorophenyl)ethan-1-amine (19), which was pure enough for use in the next step. Yield: 71%; ^{1}H NMR (400 MHz, $CDCl_3$) δ 7.25 (dd, *J* = 4.8, 8.8 Hz, 1H), 6.99 (dd, *J* = 8.0, 8.8 Hz, 1H), 4.90 (q, *J* = 6.8 Hz, 1H), 2.32 (s, 2H), 1.56 (d, *J* = 6.8 Hz, 3H).

6.3. 2-Amino-5-bromo-*N*-[1-(2,6-dichloro-3-fluorophenyl)ethyl]pyridine-3-carboxamide (8a).

2-Amino-5-bromonicotinic acid (130 mg, 0.60 mmol) was dissolved in 5 mL of DMF. The solution was cooled in an ice bath. Then to the solution were successively added HATU (228 mg, 0.66 mmol), DIPEA (126 µL, 0.72 mmol), 1-(2,6-dichloro-3-fluorophenyl)ethan-1-amine (150 mg, 0.72 mmol). The resulting solution was stirred at room temperature for 2 h and then the saturated sodium bicarbonate solution was added. The mixture was extracted with ethyl acetate (EA). The combined organic layers were dried over anhydrous Na_2SO_4 and concentrated under vacuum. The crude product was purified by flash column chromatography (0-20% EA/PE gradient) to afford 170 mg of 8**a** as a white solid (69.5% yield). ^{1}H NMR (300 MHz, DMSO-d_6) δ 9.12 (d, *J* = 5.4 Hz, 1H), 8.27 (d, *J* = 2.4 Hz, 1H), 8.15 (d, *J* = 2.4 Hz, 1H), 7.46 (dd, *J* = 5.1, 8.7 Hz, 1H), 7.36 (t, *J* = 8.7 Hz, 1H), 7.12 (s, 2H), 5.61-5.54 (m, 1H), 1.56 (d, *J* = 7.2 Hz, 3H).

6.4. 2-Amino-5-bromo-*N*-[1-(2,6-dichloro-3-fluorophenyl)ethyl]pyridine-3-sulfonamide (9a).

To the cooled 5 mL of chlorosulfonic acid at -15 ºC was added 700 mg of 2-amino-5-bromopyridine portionwise under argon. The resulting mixture was then gradually heated to 160 ºC and maintained at this temperature for 3h. After cooling, the reaction medium was slowly poured on ice and the resulting white precipitate was collected by filtration and washed with cold water to give the crude 400 mg of 2-amino-5-bromopyridine-3-sulfonyl chloride **15**, which was used immediately in the next step.

To an ice cooled solution of 1-(2,6-dichloro-3-fluorophenyl)ethan-1-amine (306 mg, 1.47 mmol) and Et_3N (205 µL, 1.47 mmol) was added **15** (400 mg, 1.47 mmol) portionwise. The resulting mixture was gradually warmed to room temperature and stirred for overnight. The reaction mixture was diluted with 10 mL of water and extracted with 10 mL of CH_2Cl_2. The organic phase was washed with brine, dried over anhydrous Na_2SO_4 and concentrated under vacuum. The crude product was purified by flash column chromatography (0-40% EA/PE gradient) to afford 374 mg of **9a** as a white solid (21% yield). ^{1}H NMR (300 MHz, DMSO-d_6) δ 8.78 (br, 1H), δ8.11 (d, *J* = 2.4 Hz, 1H), 7.48-7.24 (m, 3H), 6.77 (s, 2H), 5.19-5.12 (m, 1H), 1.50 (d, *J* = 7.2 Hz, 3H).

6.5. *N*,*N'*-dimethyl-1-[(2-nitropyridin-3-yl)oxy]methanethioamide (18).

To a solution of 2-nitropyridin-3-ol (10.00 g, 71.38 mmol) and dimethylcarbamothioic chloride (10.59 g, 85.66 mmol) in 50 mL of DMF was added DABCO (9.61 g, 85.66 mmol). The resulting mixture was stirred at room temperature for 24 h and then diluted with 150 mL of water. The resulting mixture was extracted with 600 mL of acetyl acetate. The organic layer was washed with water (3 × 100 mL), brine, dried over anhydrous Na_2SO_4 and concentrated under vacuum. The crude product as a yellow solid was pure enough for use in the next step. ^{1}H NMR (400 MHz, $CDCl_3$) δ 8.47 (dd, *J* = 2.4, 4.4 Hz, 1H), 7.77 (dd, *J* = 2.4, 8.0 Hz, 1H), 7.70 (dd, *J* = 4.4, 8.0 Hz, 1H), 3.45 (s, 3), 3.40 (s, 3H).

6.6. *N*,*N'*-dimethyl-1-[(2-nitropyridin-3-yl)sulfanyl]formamide (19).

The obtained crude product 24 was suspended in 50 mL of Ph_2O. The resulting mixture was heated at 160 ºC for 3h. After cooling, The residue was purified on silica gel column (PE/EA, 4/1-2/1) and then the crude product **19** was recrystallized from ether to afford 9.70 g of yellow solid (two steps: 60% yield). ^{1}H NMR (300 MHz, $CDCl_3$) δ 8.53 (dd, *J* = 1.8, 4.8 Hz, 1H), 8.18 (dd, *J* = 1.8, 8.1 Hz, 1H), 7.60 (dd, *J* = 4.8, 8.1 Hz, 1H), 3.12 (s, 3H), 3.04 (s, 3H).

6.7 3-{[1-(2,6-dichloro-3-fluorophenyl)ethyl]sulfanyl}pyridin-2-amine (20).

An eggplant-type flask was charged with *N*,*N'*-methyl-1-[(2-nitropyridin-3-yl)sulfanyl]formamide **25** (10.00 g, 44.01 mmol), KOH (5.43 g, 96.81 mmol). The flask was capped and then evacuated and refilled with argon three times. To the flask was added 100 mL of MeOH/THF/H_2O (2/2/1, v/v/v) via a syringe. The resulting mixture was stirred at room temperature and monitored by TLC. After the complete consumption of **25**, the organic solvents were removed under vaccum. Under argon, to the residue was add a solution of 1-(2,6-dchloro-3-fluorophenyl)ethyl methanesulfonate **12** (12.64 g, 44.61 mmol) in 120 mL of THF. The resulting medium was stirred at room temperature for another 24 h. After the

removal of the solvent by evaporation under vacuum, the residue was extracted with 300 mL of EA. The organic layer was washed with water (3 × 40 mL), brine, dried over anhydrous Na_2SO_4 and concentrated under vacuum to afford the crude product 3-{[1-(2,6-dichloro-3-fluorophenyl)ethyl]sulfanyl}-2-nitropyridine. ^{1}H NMR (300 MHz, $CDCl_3$) δ 8.36 (d, *J* = 3.9 Hz, 1H), 7.88 (d, *J* = 7.8 Hz, 1H), 7.46 (m, 1H), 7.33-7.26 (m, 1H), 7.08-7.03 (m, 1H), 5.33-5.24 (m, 1H), 1.88-1.85 (m, 3H).

The crude product 3-{[1-(2,6-dichloro-3-fluorophenyl)ethyl]sulfanyl}-2-nitropyridine was dissolved in 120 mL of EtOH. To the solution was added iron powder (12.06 g, 216.02 mmol), followed by 10 mL of HCl (1M). The resulting mixture was stirred at 80 ºC for 8 h and filtered through a pad of celite. The filtrate was concentrated under vaccum. The resulting residue was recrystallized from PE/EA (4/1). The white precipitate was collected by filtration. The corresponding filtrate was concentrated under vaccum and the residue was further purified by flash column chromatography (0-15% EA/PE gradient). The compound **20** was obtained as a white solid from **19** in 47% overall yield. ^{1}H NMR (400 MHz, $CDCl_3$) δ 8.01 (d, *J* = 4.8 Hz, 1H), 7.44-7.39 (m, 1H), 7.29-7.26 (m, 0.5H), 7.17 (dd, *J* = 4.8, 8.8 Hz, 0.5H), 7.01-6.97 (m, 1H), 6.53-6.49 (m, 1H), 5.17 (s, 2H), 5.04-4.97 (m, 1H), 1.82 (dd, *J* = 2.4, 7.2 Hz, 3H).

6.8 5-Bromo-3-{[1-(2,6-dichloro-3-fluorophenyl)ethyl]sulfanyl}pyridin-2-amine (10a).

K_2CO_3 (1.67 g, 12.05 mmol) was added to an ice-cooled solution of **20** (3.48 g, 10.96 mmol) in 25 mL of CH_2Cl_2 , followed by dropwise addition of a solution of bromine (617 μL, 12.05 mmol) in 10 mL of CH_2Cl_2. After the complete addition of bromine, the resulting mixture was stirred for an additional 5 min and quenched with saturated sodium thiosulfate solution. The mixture was extracted with CH_2Cl_2. The organic layer was washed with brine, dried over anhydrous Na_2SO_4 and concentrated under vacuum. The crude product was purified flash column chromatography (0-7% EA/PE gradient) to afford **10a** in 69% yield. ^{1}H NMR (300 MHz, $CDCl_3$) δ 8.03 (t, *J* = 2.1 Hz, 1H), 7.52 (dd, *J* = 2.4, 5.4 Hz, 1H), 7.32-7.26 (m, 0.5H), 7.21 (dd, *J* = 5.1, 9.0 Hz, 0.5H), 7.05-6.99 (m, 1H), 5.18 (s, 2H), 5.07-4.98 (m, 1H), 1.84 (dd, *J* = 2.7, 7.5 Hz, 3H).

6.9 Ethyl 2-(4-bromo-1*H*-pyrazol-1-yl)acetate (24).

To an ice-cooled solution of 4-bromo-1*H*-pyrazole (1.00 g, 6.80 mmol) in 10 mL of DMF was added portionwise sodium hydride (327 mg, 8.16 mmol, 60% percent in oil). The resulting mixture was stirred for additional 1 h. Then to the mixture was added ethyl 2-bromoacetate (0.83 mL, 7.48 mmol) and KI (226 mg, 1.36 mmol). The resulting mixture was gradually heated to 80 ºC and stirred for 8 h. After cooled to room temperature, the reaction was quenched with 20 mL of water. The mixture was extracted with EA (2 × 75 mL). The combined organic layer was washed with water (3 × 15 mL), brine (40 mL), dried over anhydrous Na_2SO_4 and concentrated under vacuum. The crude product was purified by flash column chromatography (0-10% EA/PE gradient) to afford **24** as clear colorless oil in 83% yield. ^{1}H NMR (300 MHz, $CDCl_3$) δ 7.51 (s, 2H), 4.87 (s, 2H), 4.24 (q, *J* = 6.9 Hz, 2H), 1.29 (t, *J* = 6.9 Hz, 3H).

6.10 4-Bromo-1-(oxan-4-yl)-1*H*-pyrazole (26a). Representative experimental procedure for 24 and 26b.

To an ice-cooled solution of 4-bromo-1*H*-pyrazole (1.19 g, 8.07 mmol) in 10 mL of DMF was added portionwise sodium hydride (355 mg, 8.88 mmol, 60% in oil). The resulting mixture was stirred for additional 1 h. Then to the mixture was added oxan-4-yl methanesulfonate (1.60 g, 8.88 mmol), which was prepared in a similar manner as described for **12**. The resulting mixture was gradually heated to 100 ºC and stirred for 10 h. After cooled to room temperature, the reaction was quenched with water. The mixture was extracted with EA. The organic layer was washed with brine, dried over anhydrous Na_2SO_4 and concentrated under vacuum. The crude product was purified by silica gel column chromatography (EA/PE, 1/6) to afford **33a** as white solid in 61% yield. ^{1}H NMR (300 MHz, DMSO-d_6) δ 8.06 (s, 1H), 7.55 (s, 1H), 4.41-4.35 (m, 1H), 3.95-3.92 (m, 2H), 3.47-3.40 (m, 2H), 1.95-1.87 (m, 4H).

6.11 *N,N'*-dimethyl-4-(tetramethyl-1,3,2-dioxaborolan-2-yl)-1*H*-pyrazole-1-carboxamide (25a).

To an ice-cooled solution of 4-(tetramethyl-1,3,2-dioxaborolan-2-yl)-1*H*-pyrazole (150 mg, 0.77 mmol), Et_3N (269 μL, 1.93 mmol) and catalytic amount of DMAP in 5 mL of CH_2Cl_2 was added dimethylcarbamic chloride (178 μL, 1.93 mmol). The resulting medium was stirred at room temperature for 34 h and diluted with water. The mixture was extracted with CH_2Cl_2. The organic phase was washed with brine, dried over anhydrous Na_2SO_4 and concentrated under vacuum. The crude product was purified by flash column chromatography (0-20% EA/PE gradient) o afford **25a** as a white solid in 71% yield. ^{1}H NMR (300 MHz, $CDCl_3$) δ 8.40 (s, 1H), 7.87 (s, 1H), 3.21 (s, 6H), 1.33 (s, 12H).

6.12 2-(4-Bromo-1*H*-pyrazol-1-yl)ethan-1-ol (27).

To a solution of 4-bromo-1*H*-pyrazole (1.00 g, 6.80 mmol) in 20 mL of DMF was successively added 2-bromoethanol (0.53 mL, 7.48 mmol), Cs_2CO_3 (2.66 g, 8.16 mmol) and TBAI (503 mg, 1.36 mmol). The resulting mixture was heated at 90 ºC for 2 h and diluted with 60 mL of water. The mixture was extracted with EA (3 × 100 mL). The combined organic layer was washed with water (3 × 50 mL), brine (60 mL), dried over anhydrous Na_2SO_4 and concentrated under vacuum. The crude product was purified by flash column chromatography (0-30% EA/PE gradient) o afford **27** as light yellow oil in 65% yield. ^{1}H NMR (300 MHz, $CDCl_3$) δ 7.49 (s, 1H), 7.48 (s, 1H), 4.23 (t, *J* = 4.8 Hz, 2H), 3.99 (t, *J* = 4.8 Hz, 2H), 2.73 (br, 1H).

6.13. 1-(Oxan-4-yl)-4-(tetramethyl-1,3,2-dioxaborolan-2-yl)-1*H*-pyrazole (25c). Representative experimental procedure for 25b, 25d and 25e.

To a solution of 4-bromo-1-(oxan-4-yl)-1*H*-pyrazole **33a** (1.00 g, 4.33 mmol) and 4,4,5,5-tetramethyl-2-(tetramethyl-1,3,2-dioxaborolan-2-yl)-1,3,2-dioxaborolane (1.32 g, 5.19 mmol) in 10 mL of DMF was added potassium acetate (1.27 g, 12.98 mmol), followed by *1,1'*-Bis(diphenylphosphino)ferrocene-palladium(II)dichloride dichloromethane complex (177 mg, 0.22 mmol) under argon. The resulting mixture was stirred at 80 ºC for 10 h and then diluted with 40 mL of water. The mixture was extracted with EA (3 × 30 mL). The combined organic phase was washed with water (3 × 30 mL), brine, dried over anhydrous Na_2SO_4 and concentrated under vacuum. The crude product was purified by silica gel column chromatography (EA/PE, 1/4) to afford **31c** as white solid in 68% yield. ^{1}H NMR (300 MHz, $CDCl_3$) δ 7.80 (s, 1H), 7.75 (s, 1H), 4.42-4.31 (m, 1H), 4.12-4.07 (m, 2H), 3.57-3.49 (m, 2H), 2.13-1.99 (m, 4H), 1.32 (s, 12H).

6.14. 3-{[1-(2,6-Dichloro-3-fluorophenyl)ethyl]sulfanyl}-5-[1-(oxan-4-yl)-1*H*-pyrazol-4-yl]pyridine-2-amine (10c). General experimental procedure for 8c-d and 10d-f.

A vial was charged with **10a** (200 mg, 0.50 mmol), **25c** (140 mg, 0.50 mmol), $KF{\cdot}2H_2O$ (143 mg, 1.51 mmol), $Pd(PPh_3)_4$ (29 mg, 0.25 mmol) and 5 mL of DME/H_2O/EtOH (v/v/v, 7/3/2). Then the vial was capped and heated at 110 ºC for 50 min under microwave irradiation. The reaction mixture was extracted with EA. The organic layer was washed with brine, dried over anhydrous Na_2SO_4 and concentrated under vacuum. The crude product was purified by flash column chromatography (0-3% MeOH/CH_2Cl_2 gradient) and further separated by reverse HPLC (75-80% MeOH/H_2O gradient) to afford compound **10c** in 30% yield. HPLC: 95.07 %, t_R= 3.15 min; ^{1}H NMR (300 MHz, $CDCl_3$) δ 8.12-8.11 (dd, *J* = 0.6, 2.1 Hz, 1H), 7.56 (s, 1H), 7.51-7.489 (m, 2H), 7.30-7.26 (m, 0.5H), 7.16 (dd, *J* = 5.1, 9.0 Hz, 0.5H), 7.01-6.95 (m, 1H), 5.25 (s, 2H), 5.08-5.00 (m, 1H), 4.37-4.28 (m, 1H), 4.13-4.08 (m, 2H), 3.58-3.46 (m, 2H), 2.12-2.00 (m, 4H), 1.85 (dd, *J* = 2.1, 7.5 Hz, 3H); MS (ESI, m/z): 467.0 $[M+H]^+$; HRMS (ESI) cacld for $C_{21}H_{22}Cl_2FN_4OS$ ($[M+H]^+$): 467.0875; found: 467.0891.

6.15. *tert*-Butyl 4-[4-(6-amino-5-{[1-(2,6-dichloro-3-fluorophenyl)ethyl]sulfamoyl}pyridin-3-yl)-1H-pyrazol-1-yl]piperidine-1-carboxylate (29).

To a solution of **9a** (200 mg, 0.45 mmol) and **25d** (187 mg, 0.50 mmol) in 7 mL of dioxane was added 0.68 mL of sodium carbonate solution (2 N), followed by $Pd(PPh_3)_4$ (26 mg, 0.23 mmol). The resulting mixture was evacuated and refilled with argon three times. Then the reaction mixture was heated at 80 ºC for 24 h and was extracted with 80 mL of EA. After washing with brine, the solution was dried over anhydrous Na_2SO_4 and concentrated under vacuum. The crude product was purified by flash column chromatography (0-2% MeOH/CH_2Cl_2 gradient) and further recrystallized from MeOH to afford **29** as a white solid in 40% yield. ^{1}H NMR (300 MHz, $CDCl_3$) δ: 8.11 (d, *J* = 1.5 Hz, 1H), 7.79-7.76 (m, 1H), 7.63 (s, 1H), 7.57-7.54 (m, 1H), 7.02-6.91 (m, 1H), 6.77-6.72 (m, 1H), 6.28-6.17 (m, 1H), 5.51 (s, 2H), 5.47-5.37 (m, 1H), 4.35-4.25 (m, 3H), 2.96-2.85 (m, 2H), 2.19-2.16 (m, 2H), 2.01-1.89 (m, 2H), 1.60 (d, *J* =7.2 Hz, 3H), 1.49 (s, 9H).

6.16. 2-[4-(6-Amino-5-{[1-(2,6-dichloro-3-fluorophenyl)ethyl]sulfanyl}pyridin-3-yl)-1*H*-pyrazol-1-yl]-*N*,*N'*-dimethyl acetamide (10g).

0.20 mL of 2N NaOH was added to a solution of **31** (46 mg, 0.10 mmol) , prepared in a similar manner as described for **10c**, in 2 mL of THF. The resulting medium was refluxed for 5 h. Additional 0.20 mL of 2N NaOH was added to the reaction solution. Then the reaction was stirred for another 3 h under reflux. After concentration, the remaining residue was acidified to PH 2~3 by adding 1N HCl and extracted with EA. The organic layer was dried over anhydrous Na_2SO_4 and concentrated under vacuum to give a crude acid (43 mg). The crude acid was dissolved in 2 mL of DMF and the solution was cooled in an ice bath. To the solution was successively added HATU (0.10 mmol), DIPEA (36 μL, 0.20 mmol) and dimethylamine hydrochloride (10 mg, 0.12 mmol). The resulting medium was stirred at room temperature for 1h and quenched with 2 mL of saturated $NaHCO_3$. The mixture was extracted with 50 mL of EA. The organic layer was washed with water (2 × 10 mL), brine, dried over anhydrous Na_2SO_4 and concentrated under vacuum. The crude product was purified by flash column chromatography (0-3% MeOH/EA gradient) to afford compound **10g** in 48% yield. HPLC: 96.90 %, t_R= 2.32 min; ^{1}H NMR (300 MHz, $CDCl_3$) δ 8.14 (s, 1H), 7.63 (d, *J* = 2.7 Hz, 1H), 7.60 (d, *J* = 2.7 Hz, 1H), 7.54 (dd, *J* = 2.1, 8.1 Hz, 1H), 7.32-7.26 (m, 0.5H), 7.18 (dd, *J* = 4.8, 8.7 Hz, 0.5H), 7.03-6.97 (m, 1H), 5.21 (s, 2H), 5.08-4.99 (m, 3H), 3.11 (s, 3H), 3.01 (s, 3H), 1.83 (dd, *J* = 3.3, 7.2 Hz, 3H); MS (ESI, m/z): 467.7 $[M+H]^+$; HRMS (ESI) cacld for $C_{20}H_{20}Cl_2FN_5OSNa$ ($[M+Na]^+$): 490.0647; found: 490.0630.

6.17. 3-{[1-(2,6-dichloro-3-fluorophenyl)ethyl]sulfanyl}-5-[1-(piperidin-4-yl)-1*H*-pyrazol-4-yl]pyridin-2-amine (10b). Representative experimental procedure for 8b and 9b.

To the solution of **36** (20 mg, 0.035 mmol) in 2 mL of CH_2Cl_2 was added 0.5 mL of TFA. The resulting medium was stirred at room temperature for 1h. After concentration, the residue was dissolved in CH_2Cl_2/MeOH (10/1). The solution was neutralized with saturated $NaHCO_3$ and then extracted with CH_2Cl_2. The organic phase was dried over anhydrous Na_2SO_4 and concentrated under vacuum to afford compound **10b** in 80% yield. HPLC: 97.26 %, t_R= 3.95 min; ^{1}H NMR (400 MHz, $CDCl_3$) δ 8.15-8.14 (m, 1H), 7.57 (s, 1H), 7.52 (s, 1H), 7.50-7.49 (m, 1H), 7.30 (dd, *J* = 4.8, 8.8 Hz, 0.5H), 7.18 (dd, *J* = 4.8, 8.8 Hz, 0.5H), 7.03-6.98 (m, 1H), 5.13 (s, 2H), 5.08-5.02 (m, 1H), 4.31-4.24 (m, 1H), 3.36-3.32 (m, 2H), 2.90-2.83 (m,

2H), 2.25-2.22 (m, 2H), 2.06-1.97 (m, 2H), 1.84 (dd, *J* = 3.2, 7.2 Hz, 3H); MS (ESI, m/z): 466.0 $[M+H]^+$; HRMS (ESI) cacld for $C_{21}H_{23}Cl_2FN_5OS$ ($[M+H]^+$): 466.1035; found: 466.1031.

6.18. 2-{4-[4-(Amino-5-{[1-(2,6-dichloro-3-fluorophenyl)ethyl]sulfanyl}pyridin-3-yl)-1*H*-pyrazol-yl]piperidin-1-yl}-2-oxol-ethyl acetate (32). Representative experimental procedure for 10h and 10i.

To an ice-cooled solution of **10b** (120 mg, 0.26 mmol) and Et_3N (39 μL, 0.28 mmol) in 5 mL of anhydrous CH_2Cl_2 was added dropwise 2-chloro-2-oxoethyl acetate (29 μL, 0.27 mmol). The resulting medium was stirred for additional 15 min and then diluted with 10 mL of water. The mixture was extracted with 50 mL of CH_2Cl_2. The organic phase was dried over anhydrous Na_2SO_4 and concentrated under vacuum. The crude product was purified by flash column chromatography (0-2% MeOH/CH_2Cl_2 gradient) to afford **32** in 48% yield. ^{1}H NMR (300 MHz, $CDCl_3$) δ 8.07 (s, 1H), 7.56-7.52 (m, 3H), 7.34-7.26 (m, 0.5H), 7.17 (dd, *J* = 5.1, 8.7 Hz, 0.5H), 7.04-6.99 (m, 1H), 5.78 (s, 2H), 5.07-5.03 (m, 1H), 4.78 (s, 2H), 4.70-4.66 (m, 1H), 4.41-4.34 (m, 1H), 3.86-3.82 (m, 1H), 3.26 (t, *J* = 2.4 Hz, 1H), 2.87 (t, *J* = 2.4 Hz, 1H), 2.29-2.20 (m, 5H), 2.04-1.97 (m, 2H), 1.82 (dd, *J* = 1.8, 7.5 Hz, 3H).

6.19. 1-{4-[4-(6-Amino-5-{[1-(2,6-dichloro-3-fluorophenyl)ethyl]sulfanyl}pyridin-3-yl)-1*H*-pyrazol-1-yl]piperidin-1-yl}-2-hydroxyethan-1-one (10j)

To a solution of 38 (70 mg, 0.12 mmol) in 5 mL of MeOH/H_2O (3/2) was added monohydrate lithium hydroxide (25 mg, 0.60 mmol). The resulting mixture was stirred at room temperature for 2h. After concentration, the crude product was purified by flash column chromatography (0-5% MeOH/CH_2Cl_2 gradient) to afford **10j** in 58 yield. HPLC: 95.78 %, t_R = 2.60 min; ^{1}H NMR (300 MHz, $CDCl_3$) δ 8.12 (d, *J* = 1.8Hz, 1H), 7.57 (s, 1H), 7.53 (d, *J* = 1.8 Hz, 1H), 7.51 (s, 1H), 7.31 (dd, *J* = 5.1, 8.7 Hz, 0.5H), 7.18 (dd, *J* = 5.1, 8.7 Hz, 0.5H), 7.03-6.96 (m, 1H), 5.32 (s, 2H), 5.09-5.02 (m, 1H), 4.73-4.69 (m, 1H), 4.43-4.33 (m, 1H), 4.22 (s, 2H), 3.76-3.66 (m, 1H), 3.23-3.13 (m, 1H), 3.00-2.91 (m, 1H), 2.27-2.23 (m, 2H), 2.07-1.95 (m, 2H), 1.84 (dd, *J* = 1.8, 7.5 Hz 3H); MS (ESI, m/z): 523.9 $[M+H]^+$; HRMS (ESI) cacld for $C_{23}H_{25}Cl_2FN_5O_2S$ ($[M+H]^+$): 524.1090; found: 524.1075.

6.20. Methyl 4-(6-amino-5-{[1-(2,6-dichloro-3-fluorophenyl)ethyl]sulfanyl}pyridin-3-yl)-2-fluorobenzoate (34b).

To a solution of **10a** (2.2 g, 5.55 mmol) and [3-fluoro-4-(methoxycarbonyl)phenyl]boronic acid (1.10 g, 5.55 mmol) in 44 mL of DME was added 11 mL of 1.5 M Na_2CO_3, followed by $Pd(PPh_3)_2Cl_2$ (195 mg, 0.28 mmol) under argon. The resulting mixture was stirred at 80 ºC for 16 h and extracted with EA. The organic phase was washed with brine, dried over anhydrous Na_2SO_4 and concentrated under vacuum. The crude product was purified by silica gel column chromatography (CH_2Cl_2/EA, 10/1) and further recrystallized from CH_2Cl_2 to afford **34 b** as a white solid (1.80 g, 50.6% yield). ^{1}H NMR (400 MHz, DMSO-d_6) δ 8.41 (t, *J* = 2.8 Hz, 1H), 7.86 (dt, *J* = 1.2, 8.0 Hz, 1H), 7.62-7.53 (m, 1.5H), 7.45 (dd, *J* = 1.6, 12.8 Hz, 1H), 7.39-7.32 (m, 2.5H), 6.62 (d, *J* = 3.2 Hz, 2H), 5.11-5.02 (m, 1H), 3.85 (s, 3H), 1.81 (dd, *J* = 1.6, 7.6 Hz, 3H).

6.21. 4-(6-Amino-5-{[1-(2,6-dichloro-3-fluorophenyl)ethyl]sulfanyl}pyridin-3-yl)-2-fluorobenzoic acid (35b).

40b (1.00 g, 2.13 mmol) was suspended in 20 mL of MeOH/THF/H_2O (2/1/1). To this suspension was added $LiOH{\cdot}H_2O$ (447 mg, 10.65 mmol). The resulting mixture was stirred at room temperature for 10 h. After concentration, the residue was acidified to PH 2~3 by adding 1N HCl. The white precipitate was filtered and dried to afford **35b** as a white solid (900 mg, 93% yield). ^{1}H NMR (400 MHz, DMSO-d_6) δ 13.16 (br, 1H), 8.41 (t, *J* = 2.4 Hz, 1H), 7.85 (t, *J* = 8.0 Hz, 1H), 7.63 (d, *J* = 16.0 Hz, 1H), 7.56 (dd, *J* = 5.2, 8.8 Hz, 0.5H), 7.44-7.32 (m, 3.5H), 6.78 (s, 2H), 5.10-5.04 (m, 1H), 1.82 (dd, *J* = 2.4, 7.2 Hz, 3H).

6.22. 4-(6-Amino-5-{[1-(2,6-dichloro-3-fluorophenyl)ethyl]sulfanyl}pyridin-3-yl)-2-fluoro-*N,N'*-dimethylbenzamide (36k). Representative experimental procedure for 36i, 36j and 36l.

To an ice-cooled suspension of **35b** (120 mg, 0.26 mmol) in 4 mL of CH_2Cl_2 was successively added EDCI (56 mg, 0.29 mmol), HOBT (39 mg, 0.29 mmol), Et_3N (40 μL, 0.29 mmol) and 316 μL of dimethyl amine (2M solution in THF). The resulting mixture was stirred at room temperature for 6 h and quenched with saturated sodium carbonate solution. The mixture was extracted with CH_2Cl_2. The organic phase was washed with brine, dried over anhydrous Na_2SO_4 and concentrated under vacuum. The crude product was purified by flash column chromatography (60-70% EA/PE gradient) to afford **36k** in 69% yield. HPLC: 98.08 %, t_R= 3.46 min; ^{1}H NMR (400 MHz, $CDCl_3$) δ 8.22 (s, 1H), 7.60 (s, 1H), 7.40 (t, *J* = 7.6 Hz, 1H), 7.31-7.27 (m, 0.5H), 7.23-7.13 (m, 1.5H), 7.07 (d, *J* = 10.8 Hz, 1H), 7.02-6.96 (m, 1H), 5.44 (s, 2H), 5.10-4.99 (m, 1H), 3.13 (s, 3H), 2.96 (s, 3H), 1.85-1.82 (m, 3H); EI-MS *m/z* (M^+) 481; EI-HRMS calcd for (M^+) 481.0594, found: 481.0588.

6.23. (1*S*)-1-(2,6-Dichloro-3-fluorophenyl)ethan-1-ol (38).

1-(2,6-Dichloro-3-fluorophenyl)ethan-1-ol **37** (24.00 g, 114.81 mmol) was dissolved in 300 mL of CH_2ClCH_2Cl. The solution was cooled to -5 .To the solution was successively added Boc-L-proline (16.06 g, 74.63 mmol), EDCI (17.61 g, 91.85 mmol) and DMAP (1.68 g, 13.78 mmol). The resulting mixture was continued to stir overnight and diluted with 100 mL of water. The organic layer was collected, washed with brine, dried over anhydrous Na_2SO_4 and concentrated under

vacuum. The crude product was purified by silica gel column chromatography (PE/EA 100/1-50/1, v/v) to afford (1*S*)-1-(2,6-dichloro-3-fluorophenyl)ethan-1-ol. (7.00 g, 58% yield). ^{1}H NMR (400 MHz, $CDCl_3$) δ 7.26 (dd, *J* = 4.8, 8.8 Hz, 1H), 7.02 (dd, *J* = 8.0, 8.8 Hz, 1H), 5.57 (q, *J* = 6.8 Hz, 1H), 2.86 (s, 1H), 1.64 (d, *J* = 6.8 Hz, 3H).

6.24. (1*S*)-1-(2,6-Dichloro-3-fluorophenyl)ethyl methanesulfonate ((*S*)-12).

(*S*)-**12** was prepared in a similar manner as described for compound **12.** ^{1}H NMR (400 MHz, $CDCl_3$) δ 7.33 (dd, *J* = 4.8, 8.8 Hz, 1H), 7.12 (dd, *J* = 8.0, 8.8 Hz, 1H), 6.45 (q, *J* = 6.8 Hz, 1H), 2.91 (s, 3H), 1.84 (d, *J* = 6.8 Hz, 3H).

6.25. 5-Bromo-3-{[(1*R*)-1-(2,6-dichloro-3-fluorophenyl)ethyl]sulfanyl}pyridin-2-amine ((*R*)-10a).
(*R*)-**10a** was prepared in a similar manner as described for compound **10a.** ^{1}H NMR (400 MHz, $CDCl_3$) δ 8.04-8.02 (m, 1H), 7.51 (dd, *J* = 2.4, 7.6 Hz, 1H), 7.29 (dd, *J* = 4.8, 8.8 Hz, 0.5H), 7.20 (dd, *J* = 4.8, 8.8 Hz, 0.5H), 7.04-6.99 (m, 1H), 5.16 (s, 2H), 5.06-4.98 (m, 1H), 1.83 (dd, *J* = 3.6, 7.2 Hz, 3H).

6.26. *tert*-Butyl-[4-(6-amino-5-{[(1*R*)-1-(2,6-dichloro-3-fluorophenyl)ethyl]sulfanyl}pyridine-3-yl)-1*H*-pyrazol-1-yl]piperidine-1-carboxylate ((*R*)-30).
To a solution of **42** (2.40 g, 6.06 mmol) and **26d** (2.51 g, 6.66 mmol) in 48 mL of DMF was added 12 mL of 1.5 M Na_2CO_3, followed by $Pd(dppf)_2Cl_2$ (247 mg, 0.30 mmol) under argon. The resulting mixture was stirred at 80 for 10 h and extracted with EA. The organic phase was washed with brine, dried over anhydrous Na_2SO_4 and concentrated under vacuum. The crude product was purified by reverse HPLC (MeOH/H_2O, 10/1) to afford **43** as a white solid (1.70 g, 48.4% yield). ^{1}H NMR (400 MHz, $CDCl_3$) δ 8.13-8.10 (m, 1H), 7.56 (s, 1H), 7.53-7.48 (m, 2H), 7.29 (dd, *J* = 5.2, 8.8 Hz, 0.5H), 7.17 (dd, *J* = 5.0, 8.8 Hz, 0.5H), 5.24 (s, 2H), 5.09-5.02 (m, 1H), 4.41-4.16 (m, 3H), 2.99-2.78 (m, 2H), 2.18-2.10 (m, 2H), 1.98-1.87 (m, 2H), 1.84 (dd, *J* = 3.2, 7.2 Hz, 3H), 1.48 (s, 12H).

6.27. 3-{[(1*R*)-1-(2,6-dichloro-3-fluorophenyl)ethyl]sulfanyl}-5-[1-(piperidin-4-yl)-1*H*-pyrazol-4-yl]pyridin-2-amine ((*R*)-10b).
(*R*)-**10b** was prepared in a similar manner as described for compound **10b.** $[\alpha]_D^{18}$ +177 (C = 0.047, MeOH); ^{1}H NMR (400 MHz, $CDCl_3$) δ 8.12 (t, *J* = 2.0 Hz, 1H), 7.57 (s, 1H), 7.52 (s, 1H), 7.19 (t, *J* = 2.4 Hz, 1H), 7.30 (dd, *J* = 4.8, 8.8 Hz, 0.5H), 7.18 (dd, *J* = 4.8, 8.8 Hz, 0.5H), 7.02-6.98 (m, 1H), 5.16 (s, 2H), 5.09-5.02 (m, 1H), 4.26-4.19 (m, 1H), 3.29-3.26 (m, 2H), 2.83-2.76 (m, 2H), 2.19-2.14 (m, 2H), 1.98-1.88 (m, 2H), 1.83 (dd, *J* = 3.2, 7.2 Hz, 3H); ^{13}C NMR (100 MHz, $CDCl_3$) δ 159.03, 158.47, 157.95, 156.56, 155.47, 146.25, 146.14, 142.21, 139.75, 139.69, 135.70, 130.38, 130.30, 130.09, 130.06, 129.47, 129.44, 128.64, 128.57, 123.06, 122.86, 122.70, 122.67, 122.47, 122.29, 120.02, 119.97, 119.03, 115.80, 115.75, 115.56, 115.52, 112.54, 59.77, 45.63, 45.38, 44.68, 33.85, 29.76, 19.30; MS (ESI, m/z): 466.1 $[M+H]^+$.

Acknowledgments

HCC827and HCC827/GR6 were kindly gifted by Dr. Pasi A. Jänne (Dana-Farber Cancer Institute, Boston, MA). We gratefully acknowledge financial support from National Basic Research Program of China (Grants 2009CB940903 and 2012CB518000), the National Natural Science Foundation of China (Grants 20721003 and 81025017), National S&T Major Projects (2012ZX09103-101-072) and Silver Project (260644).National Science & Technology Major Project "Key New Drug Creation and Manufacturing Program" (No.2012ZX09301001-007), National Program on Key Basic Research Project of China (No.2012CB910704), the Natural Science Foundation of China for Innovation Research Group (No.81021062) and the National Natural Science Foundation (No. 81102461).

References and notes

(1) Gherardi, E.; Birchmeier, W.; Birchmeier, C.; Woude, G. V. *Nat. Rev. Cancer.* **2012***, 12, 89-103.*
(2) Birchmeier, C.; Birchmeier, W.; Gherardi, E.; Vande Woude, G. F. *Nat. Rev. Mol. Cell Biol.* **2003**, *4*, 915-925.
(3) Comoglio, P. M.; Giordano, S.; Trusolino, L. *Nat. Rev. Drug Discov.* **2008**, *7*, 504-516.
(4) Liu, X. D.; Newton, R. C.; Scherle, P. A. Tr*ends Mol. Med.* **2010**, *16*, 37-45.
(5) Schoffski, P.; Garcia, J. A.; Stadler, W. M.; Gil, T.; Jonasch, E.; Tagawa, S. T.; Smitt, M.; Yang, X. Q.; Oliner, K. S.; Anderson, A.; Zhu, M.; Kabbinavar, F. *Bju Int.* **2011**, *108*, 679-686.
(6) Lu, R. M.; Chang, Y. L.; Chen, M. S.; Wu, H. C. *Biomaterials.* **2011**, *32*, 3265-3274.
(7) Pacchiana, G.; Chiriaco, C.; Stella, M. C.; Petronzelli, F.; De Santis, R.; Galluzzo, M.; Carminati, P.; Comoglio, P. M.; Michieli, P.; Vigna, E. *J. Biol. Chem.* **2010**, *285*, 36149-36157.
(8) Liu, L.; Zeng, W.; Wortinger, M.; Uhlik, M. T.; Stewart, J.; Tetreault, J.; Lu, J.; Vaillancourt, P.; Tang, Y.; Wooldridge, J. *Ejc Suppl.* **2010**, *8*, 74-75.

(9) Okamoto, W.; Okamoto, I.; Tanaka, K.; Hatashita, E.; Yamada, Y.; Kuwata, K.; Yamaguchi, H.; Arao, T.; Nishio, K.; Fukuoka, M.; Janne, P. A.; Nakagawa, K. *Mol. Cancer. Ther.* **2010**, *9*, 2785-2792.
(10) Schelter, F.; Kobuch, J.; Moss, M. L.; Becherer, J. D.; Comoglio, P. M.; Boccaccio, C.; Kruger, A. *J. Biol. Chem.* **2010**, *285*, 26335-26340.
(11) Giordano, S. *Curr. Opin. Mol. Ther.* **2009**, *11*, 448-455.
(12) van der Horst, E.; Chinn, L.; Wang, M.; Velilla, T.; Tran, H.; Madrona, Y.; Lam, A.; Ji, M.; Hoey, T. C.; Sato, A. K. *Neoplasia.* **2009**, *11*, 355-364.
(13) Perk, L. R.; Walsum, M. S. V.; Visser, G. W. M.; Kloet, R. W.; Vosjan, M. J. W. D.; Leemans, C. R.; Giaccone, G.; Albano, R.; Comoglio, P. M.; van Dongen, G. A. M. S. *Eur J. Nucl. Med Mol. Imaging.* **2008**, *35*, 1857-1867.
(14) Jin, H. K.; Yang, R. H.; Zheng, Z.; Romero, M.; Ross, J.; Bou-Reslan, H.; Carano, R. A. D.; Kasman, I.; Mai, E.; Young, J.; Zha, J. P.; Zhang, Z. M.; Ross, S.; Schwall, R.; Colbern, G.; Merchant, M. *Cancer Res.* **2008**, *68*, 4360-4368.
(15) Bottaro, D. P. *Ann Oncol.* **2008**, *19*, 22-22.
(16) Martens, T.; Schmidt, N. O.; Eckerich, C.; Fillbrandt, R.; Merchant, M.; Schwall, R.; Westphal, M.; Lamszus, K. *Clin. Cancer Res.* **2006**, *12*, 6144-6152.
(17) Welsh, J.; Zhan, Y.; Likhacheva, A.; Komaki, R. *Ejc Suppl.* **2010**, *8*, 162-162.
(18) Youles, M.; Holmes, O.; Petoukhov, M. V.; Nessen, M. A.; Stivala, S.; Svergun, D. I.; Gherardi, E. *J. Mol. Biol.* **2008**, *377*, 616-622.
(19) Raymond, W. W.; Cruz, A. C.; Caughey, G. H. *J. Biol. Chem.* **2006**, *281*, 1489-1494.
(20) Atabey, N.; Gao, Y.; Yao, Z. J.; Breckenridge, D.; Soon, L.; Soriano, J. V.; Burke, T. R.; Bottaro, D. P. *J. Biol. Chem.* **2001**, *276*, 14308-14314.
(21) Schwall, R. H.; Chang, L. Y.; Godowski, P. J.; Kahn, D. W.; Hillan, K. J.; Bauer, K. D.; Zioncheck, T. F. *J. Cell. Biol.* **1996**, *133*, 709-718.
(22) Chen, F.; Wang, Y.; Ai, J.; Zhan, Z.; Lv, Y.; Liang, Z.; Luo, C.; Mei, D.; Geng, M.; Duan, W. *Chem. Med. Chem.* **2012**, *7*, 1276-1285.
(23) Cui, J. J.; McTigue, M.; Nambu, M.; Tran-Dubé, M.; Pairish, M.; Shen, H.; Jia, L.; Cheng, H.; Hoffman, J.; Le, P.; Jalaie, M.; Goetz, G. H.; Ryan, K.; Grodsky, N.; Deng, Y.-l.; Parker, M.; Timofeevski, S.; Murray, B. W.; Yamazaki, S.; Aguirre, S.; Li, Q.; Zou, H.; Christensen, J. *J. Med. Chem.* **2012**, *55*, 8091-8109.
(24) Wang, Y.; Ai, J.; Wang, Y.; Chen, Y.; Wang, L.; Liu, G.; Geng, M.; Zhang, A. *J. Med. Chem.* **2011**, *54*, 2127-2142.
(25) Katz, J. D.; Jewell, J. P.; Guerin, D. J.; Lim, J.; Dinsmore, C. J.; Deshmukh, S. V.; Pan, B. S.; Marshall, C. G.; Lu, W.; Altman, M. D.; Dahlberg, W. K.; Davis, L.; Falcone, D.; Gabarda, A. E.; Hang, G.; Hatch, H.; Holmes, R.; Kunii, K.; Lumb, K. J.; Lutterbach, B.; Mathvink, R.; Nazef, N.; Patel, S. B.; Qu, X.; Reilly, J. F.; Rickert, K. W.; Rosenstein, C.; Soisson, S. M.; Spencer, K. B.; Szewczak, A. A.; Walker, D.; Wang, W.; Young, J.; Zeng, Q. *J. Med. Chem.* **2011,** *54*, 4092-4108.
(26) Cui, J. J.; Tran-Dube, M.; Shen, H.; Nambu, M.; Kung, P. P.; Pairish, M.; Jia, L.; Meng, J.; Funk, L.; Botrous, I.; McTigue, M.; Grodsky, N.; Ryan, K.; Padrique, E.; Alton, G.; Timofeevski, S.; Yamazaki, S.; Li, Q. H.; Zou, H. L.; Christensen, J.; Mroczkowski, B.; Bender, S.; Kania, R. S.; Edwards, M. P. *J. Med. Chem.* **2011**, *54*, 6342-6363.
(27) Williams, D. K.; Chen, X. T.; Tarby, C.; Kaltenbach, R.; Cai, Z. W.; Tokarski, J. S.; An, Y. M.; Sack, J. S.; Wautlet, B.; Gullo-Brown, J.; Henley, B. J.; Jeyaseelan, R.; Kellar, K.; Manne, V.; Trainor, G. L.; Lombardo, L. J.; Fargnoli, J.; Borzilleri, R. M. *Bioorg. Med. Chem. Lett.* **2010**, *20*, 2998-3002.
(28) Cho, S. Y.; Han, S. Y.; Ha, J. D.; Ryu, J. W.; Lee, C. O.; Jung, H.; Kang, N. S.; Kim, H. R.; Koh, J. S.; Lee, J. *Bioorg. Med. Chem. Lett.* **2010**, *20*, 4223-4227.
(29) Schroeder, G. M.; An, Y. M.; Cai, Z. W.; Chen, X. T.; Clark, C.; Cornelius, L. A. M.; Dai, J.; Gullo-Brown, J.; Gupta, A.; Henley, B.; Hunt, J. T.; Jeyaseelan, R.; Kamath, A.; Kim, K.; Lippy, J.; Lombardo, L. J.; Manne, V.; Oppenheimer, S.; Sack, J. S.; Schmidt, R. J.; Shen, G.; Stefanski, K.; Tokarski, J. S.; Trainor, G. L.; Wautlet, B. S.; Wei, D.; Williams, D. K.; Zhang, Y. R.; Zhang, Y. P.; Fargnoli, J.; Borzilleri, R. M. *J. Med. Chem.* **2009**, *52*, 1251-1254.
(30) Raeppel, S.; Claridge, S.; Saavedra, O.; Gaudette, F.; Zhan, L. J.; Mannion, M.; Zhou, N.; Raeppel, F.; Granger, M. C.; Isakovic, L.; Deziel, R.; Nguyen, H.; Beaulieu, N.; Beaulieu, C.; Dupont, I.; Robert, M. F.; Lefebvre, S.; Dubay, M.; Rahil, J.; Wang, J.; Ste-Croix, H.; Macleod, A. R.; Besterman, J.; Vaisburg, A. *Bioorg. Med. Chem. Lett.* **2009**, *19*, 1323-1328.
(31) Porter, J.; Lumb, S.; Lecomte, F.; Reuberson, J.; Foley, A.; Calmiano, M.; le Riche, K.; Edwards, H.; Delgado, J.; Franklin, R. J.; Gascon-Simorte, J. M.; Maloney, A.; Meier, C.; Batchelor, M. *Bioorg. Med. Chem. Lett.* **2009**, *19*, 397-400.
(32) Porter, J.; Lumb, S.; Franklin, R. J.; Gascon-Simorte, J. M.; Calmiano, M.; Le Riche, K.; Lallemand, B.; Keyaerts, J.; Edwards, H.; Maloney, A.; Delgado, J.; King, L.; Foley, A.; Lecomte, F.; Reuberson, J.; Meier, C.; Batchelor, M. *Bioorg. Med. Chem. Lett.* **2009**, *19*, 2780-2784.
(33) Mannion, M.; Raeppel, S.; Claridge, S.; Zhou, N.; Saavedra, O.; Isakovic, L.; Zhan, L. J.; Gaudette, F.; Raeppel, F.; Deziel, R.; Beaulieu, N.; Nguyen, H.; Chute, I.; Beaulieu, C.; Dupont, I.; Robert, M. F.; Lefebvre, S.; Dubay, M.; Rahil, J.; Wang, J.; Ste-Croix, H.; Macleod, A. R.; Besterman, J. M.; Vaisburg, A. *Bioorg. Med. Chem. Lett.* **2009**, *19*, 6552-6556.
(34) Koolman, H.; Heinrich, T.; Boettcher, H.; Rautenberg, W.; Reggelin, M. *Bioorg. Med. Chem. Lett.* **2009**, *19*, 1879-1882.

(35) Boezio, A. A.; Berry, L.; Albrecht, B. K.; Bauer, D.; Bellon, S. F.; Bode, C.; Chen, A.; Choquette, D.; Dussault, I.; Hirai, S.; Kaplan-Lefko, P.; Larrow, J. F.; Lin, M. H. J.; Lohman, J.; Potashman, M. H.; Rex, K.; Santostefano, M.; Shah, K.; Shimanovich, R.; Springer, S. K.; Teffera, Y.; Yang, Y. J.; Zhang, Y. H.; Harmange, J. C. *Bioorg. Med. Chem. Lett.* **2009**, *19*, 6307-6312.
(36) Schroeder, G. M.; Chen, X. T.; Williams, D. K.; Nirschl, D. S.; Cai, Z. W.; Wei, D.; Tokarski, J. S.; An, Y. M.; Sack, J.; Chen, Z.; Huynh, T.; Vaccaro, W. N.; Poss, M.; Wautlet, B.; Gullo-Brown, J.; Kellar, K.; Manne, V.; Hunt, J. T.; Wong, T. W.; Lombardo, L. J.; Fargnoli, J.; Borzilleri, R. M. *Bioorg. Med. Chem. Lett.* **2008**, *18*, 1945-1951.
(37) Liu, L. B.; Siegmund, A.; Xi, N.; Kaplan-Lefko, P.; Rex, K.; Cheti, A.; Lin, J.; Moriguchi, J.; Berry, L.; Huang, L.; Teffera, Y.; Yang, Y. I.; Zhang, Y. H.; Bellon, S. F.; Lee, M.; Shimanovich, R.; Bak, A.; Dominguez, C.; Norman, M. H.; Harmange, J. C.; Dussault, I.; Kimt, T. S. *J. Med. Chem.* **2008**, *51*, 3688-3691.
(38) Kim, K. S.; Zhang, L. P.; Schmidt, R.; Cai, Z. W.; Wei, D.; Williams, D. K.; Lombardo, L. J.; Trainor, G. L.; Xie, D. L.; Zhang, Y. Q.; An, Y. M.; Sack, J. S.; Tokarski, J. S.; Darienzo, C.; Kamath, A.; Marathe, P.; Zhang, Y. P.; Lippy, J.; Jeyaseelan, R.; Wautlet, B.; Henley, B.; Gullo-Brown, J.; Manne, V.; Hunt, J. T.; Fargnoli, J.; Borzilleri, R. M. *J. Med. Chem.* **2008**, *51*, 5330-5341.
(39) D'Angelo, N. D.; Bellon, S. F.; Booker, S. K.; Cheng, Y.; Coxon, A.; Dominguez, C.; Fellows, I.; Hoffman, D.; Hungate, R.; Kaplan-Lefko, P.; Lee, M. R.; Li, C.; Liu, L. B.; Rainbeau, E.; Reider, P. J.; Rex, K.; Siegmund, A.; Sun, Y. X.; Tasker, A. S.; Xi, N.; Xu, S. M.; Yang, Y. J.; Zhang, Y. H.; Burgess, T. L.; Dussault, I.; Kim, T. S. *J. Med. Chem.* **2008**, *51*, 5766-5779.
(40) Cai, Z. W.; Wei, D.; Schroeder, G. M.; Cornelius, L. A. M.; Kim, K.; Chen, X. T.; Schmidt, R. J.; Williams, D. K.; Tokarski, J. S.; An, Y. M.; Sack, J. S.; Manne, V.; Kamath, A.; Zhang, Y. P.; Marathe, P.; Hunt, J. T.; Lombardo, L. J.; Fargnoli, J.; Borzilleri, R. M. *Bioorg. Med. Chem. Lett.* **2008**, *18*, 3224-3229.
(41) Albrecht, B. K.; Harmange, J. C.; Bauer, D.; Berry, L.; Bode, C.; Boezio, A. A.; Chen, A.; Choquette, D.; Dussault, I.; Fridrich, C.; Hirai, S.; Hoffman, D.; Larrow, J. F.; Kaplan-Lefko, P.; Lin, J.; Lohman, J.; Long, A. M.; Moriguchi, J.; O'Connor, A.; Potashman, M. H.; Reese, M.; Rex, K.; Siegmund, A.; Shah, K.; Shimanovich, R.; Springer, S. K.; Teffera, Y.; Yang, Y.; Zhang, Y.; Bellon, S. F. *J. Med. Chem.* **2008**, *51*, 2879-2882.
(42) Underiner, T. L.; Herbertz, T.; Miknyoczki, S. J. *Anti-Cancer. Agent. Me.* **2010**, *10*, 7-27.
(43) Lauffer, D.; Li, P.; McGinty, K.; Ronkin, S.; Tang, Q.; Grillot, A-L.; Waal, N. PCT Int. Appl. WO2010048131, 2010.
(44) (a) Mulvihill, M. J.; Wang, J.; Chen, X.; Wang, T.; Li, A. H.; Steinig, A. G.; Kleinberg, A.; Weng, Q. H.; Dong, H. Q; Jin, M. Z. PCT Int. Appl. WO2009100282, 2009. (b) Chen, X.; Jin, M. Z.; Kleinberg, A.; Li, A. H.; Mulvihill, M. J.; Steinig, A. G; Wang, J. PCT Int. Appl. WO2010059771, 2010.
(45) Barlaam, B. C.; Chuaqui, C. E.; Delouvrie, B.; Ouvry, G.; Wang, T.; Winter, J. J. G. PCT Int. Appl. WO2009024825, 2009.
(46) Barlaam, B. C.; Bower, J. F.; Delouvrie, B.; Fairley, G.; Harris, C. S.; Lambert, C.; Ouvry, G.; Winter, J. J. G. PCT Int. Appl. WO2009053737, 2009.
(47) Liang, C. X. PCT Int. Appl. WO2008088881, 2008.
(48) Viviani, F.; Vors, J. P.; Gaudry, M.; Marquet, A. Bull. Soc. Chim. Fr. **1993** , *130*, 395 - 404
(49) Lin, W. Q.; Zhang, X. M.; He, Z.; Jin, Y.; Gong, L. Z.; Mi, A. Q. Synth. Commun. **2002**, *32*, 3279-3284.
(50) Bernard, P.; Raogo, O.; Pascal, d. T.; Smail, K.; Fabian, S.; Stéphane, B.; Léon, D.; Jeanine, F.; Jacques, D.; Philippe, L. *J. Med. Chem.* **2000**, *43*, 1456-1466
(51) Engelman, J. A.; Zejnullahu, K.; Mitsudomi, T.; Song, Y.; Hyland, C.; Park, J. O.; Lindeman, N.; Gale, C. M.; Zhao, X.; Christensen, J.; Kosaka, T.; Holmes, A. J.; Rogers, A. M.; Cappuzzo, F.; Mok, T.; Lee, C.; Johnson, B. E.; Cantley, L. C.; Jänne, P. A. Science. **2007**, *316*, 1039-1043.

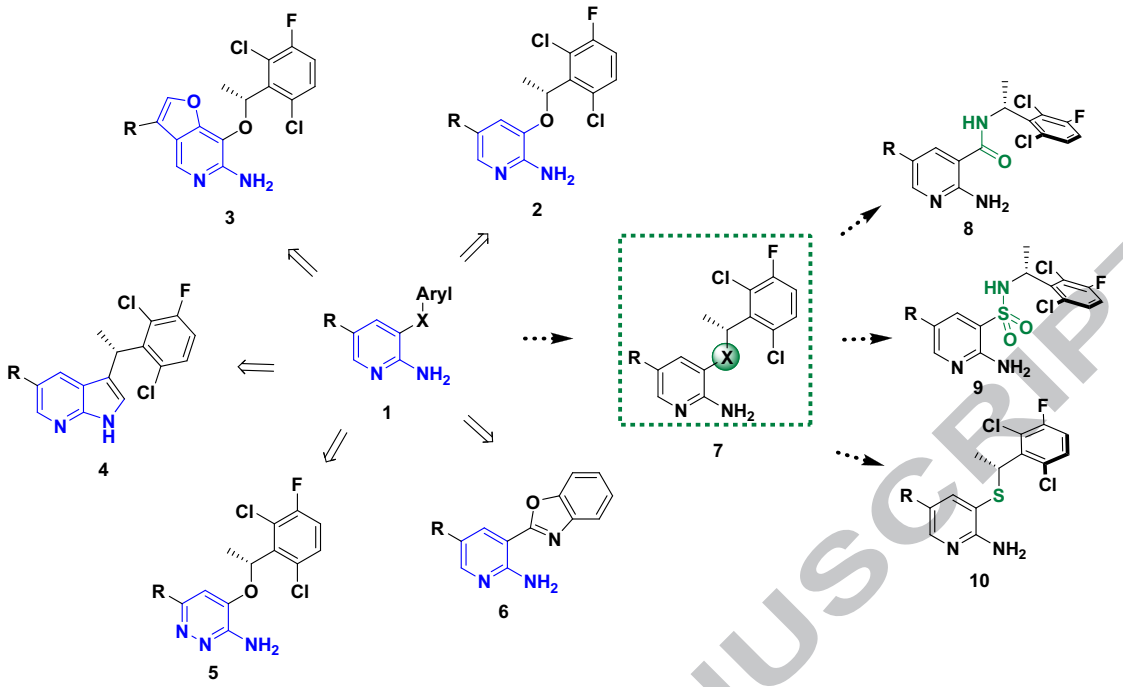

Figure 1. Representive modifications of the aminopyridine based c-Met inhibitors.

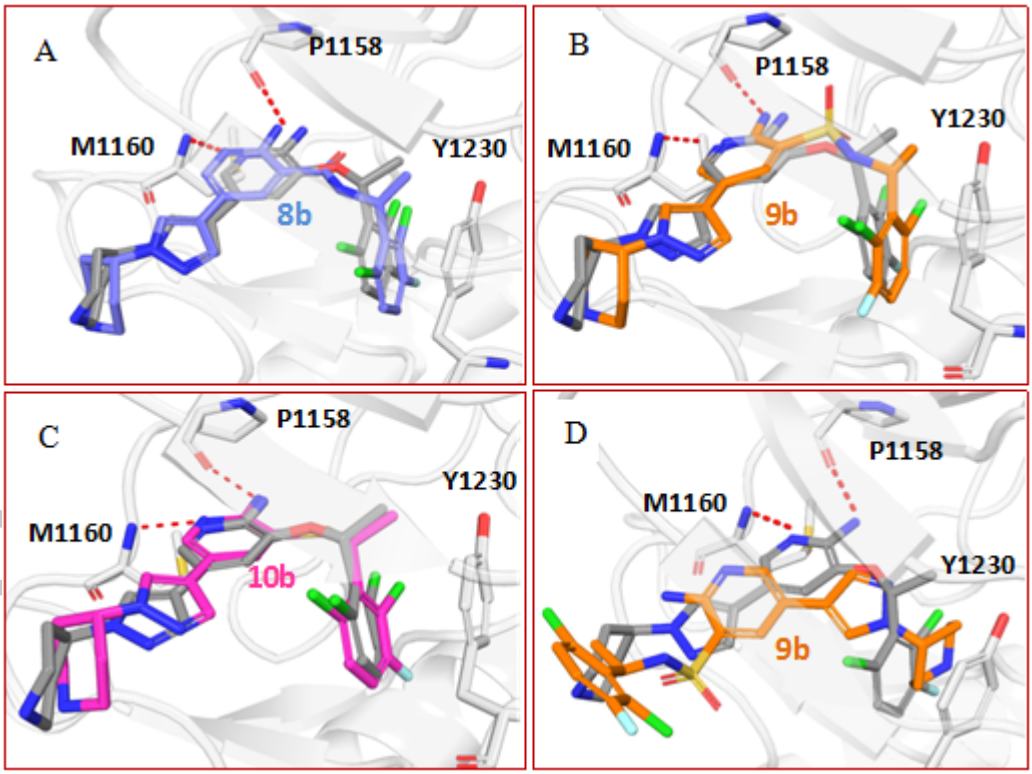

Figure 2. The binding model comparison of designed compounds with crizotinib. A. Binding pose of compound **8b** with c-Met; B and D. Binding pose of compound **9b** with c-Met; C. Binding pose of compound **10b** with c-Met.

Scheme 1. Synthesis of 2-amino-*N*-benzyl-5-bromopyridine-3-carboxamide core 8a[a]

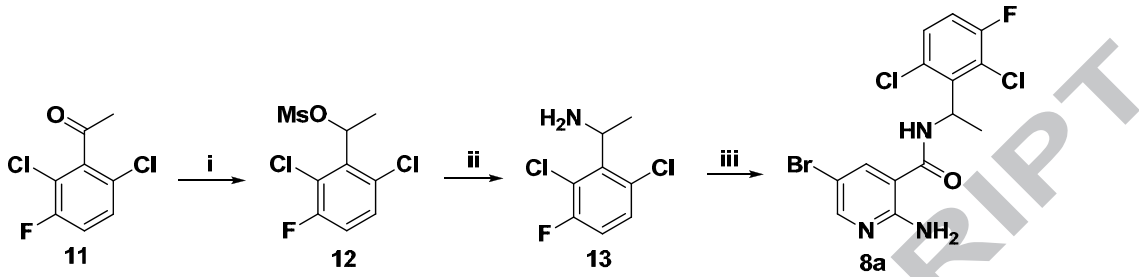

[a] Reagents and conditions: (**i**) $NaBH_4$, MeOH, rt; MsCl, Et_3N, 0 ºC -rt, 84% (2 steps) ; (**ii**) NaN_3, DMF, 50 ºC; Zn, NH_4Cl, EtOH/H_2O (3:1), rt, 71%; (2 steps); (**iii**) 2-amino-5-bromopyridine-3-carboxylic acid, HATU, DIPEA, DMF, 0 ºC-rt, 70%.

Scheme 2. Synthesis of 2-amino-*N*-benzyl-5-bromopyridine-3-sulfonamide core 9a[a]

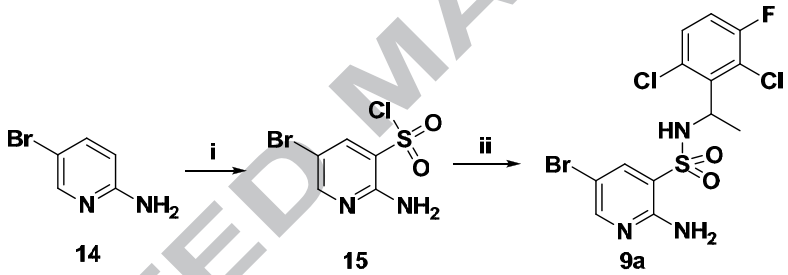

[a] Reagents and conditions: (**i**) $ClSO_3H$, -15 ºC-160 ºC; (**ii**) **13**, CH_2Cl_2, Et_3N, 0 ºC-rt, 21% (2 steps).

Scheme 3. Synthesis of 3-(benzylsulfanyl)-5-bromopyridin-2-amine core 10a[a]

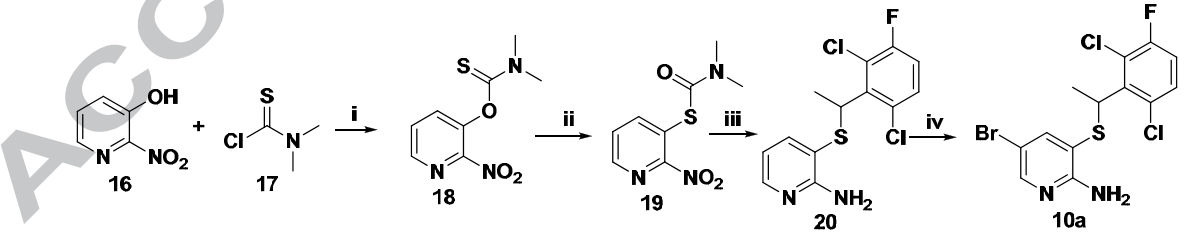

[a] Reagents and conditions: (**i**) DABCO, DMF, rt, 24h; (**ii**) Ph_2O, 160 ºC, 3h; (**iii**) **12**, KOH, MeOH/THF/H_2O (2:1:1), 0 ºC -rt; Fe/HCl, EtOH, reflux, 47% (3 steps); (**iv**) Br_2, K_2CO_3, CH_2Cl_2, 0 ºC, 69%.

Scheme 4. Synthesis of pyrazolyl-4-boronic ester[a]

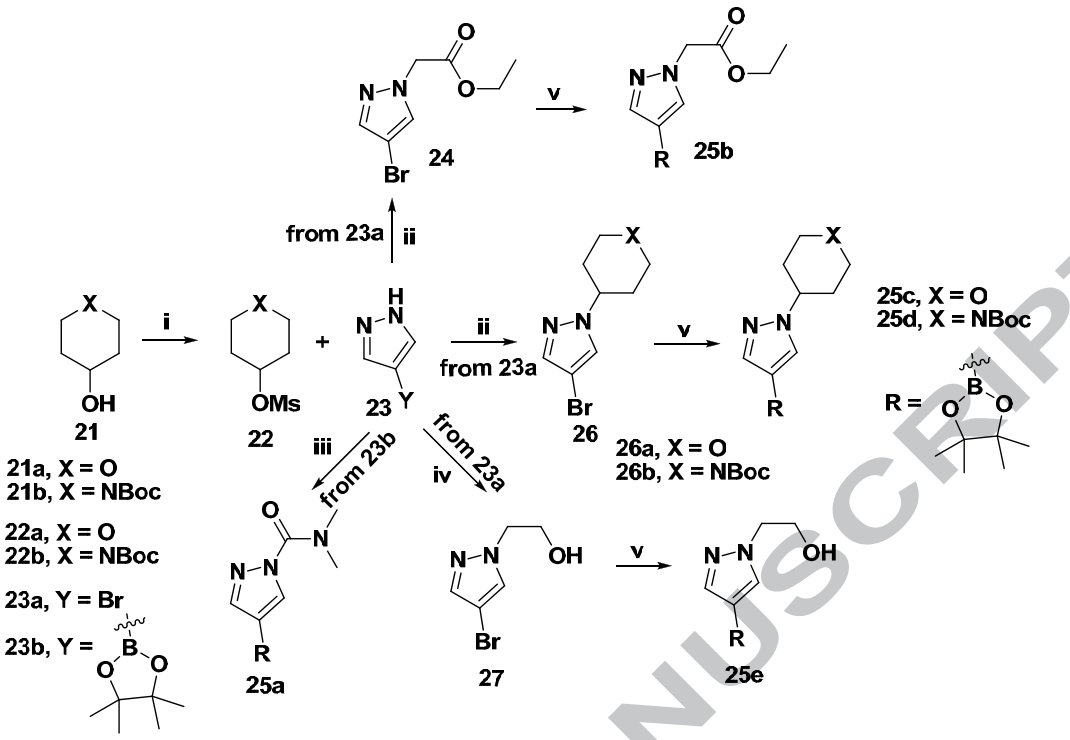

[a] Reagents and conditions: (**i**) MsCl, Et_3N, DMAP, CH_2Cl_2, 0 ºC-rt, 94%; (**ii**) NaH, DMF, 0 ºC -100 ºC, 61-83%; (**iii**) dimethylcarbamic chloride, Et_3N, DMAP, CH_2Cl_2, rt, 71%; (**iv**) 2-bromoethanol, Cs_2CO_3, TBAI, DMF, 90 ºC, 65%; (**v**) Bis(pinacolato)diboron, $Pd(dppf)Cl_2$, AcOK, DMF, 80 ºC, 8-73%.

Scheme 5. Synthesis of compounds 8b-d, 9b, 10b-j[a]

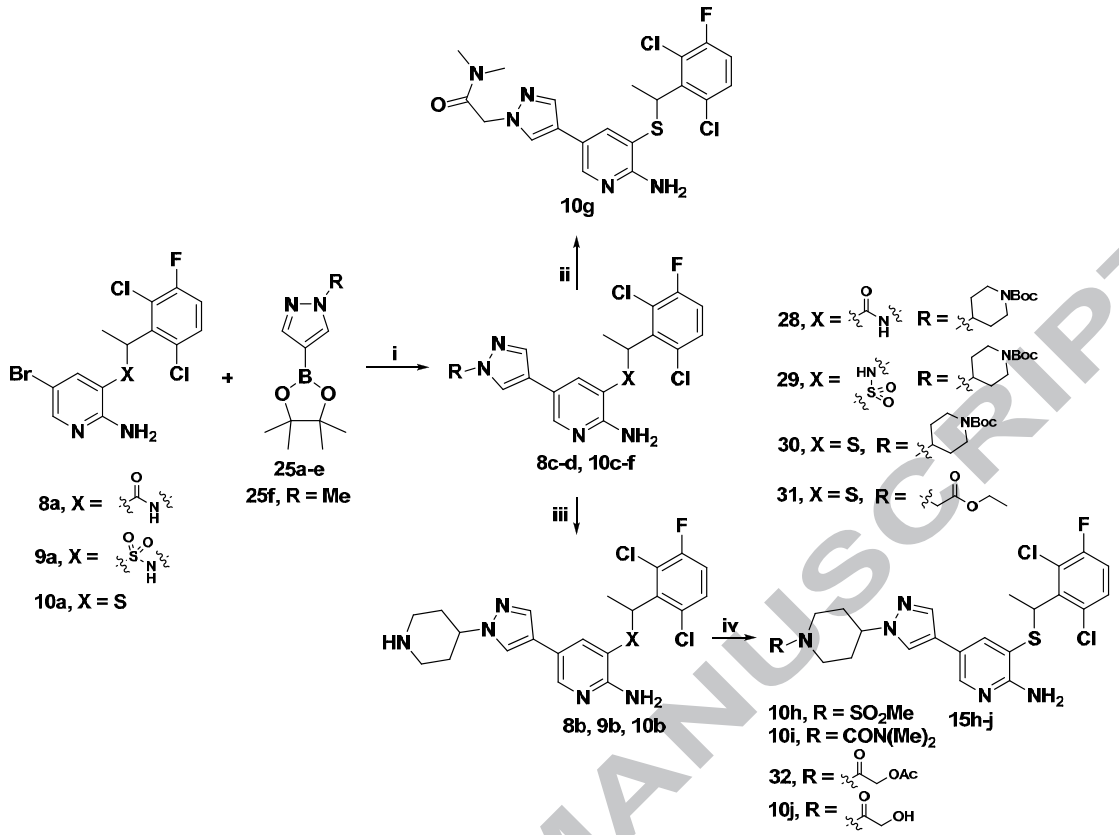

[a] Reagents and conditions: (i) For **8a** and **10a**, $Pd(PPh_3)_4$, $KF{\cdot}2H_2O$, DME/H_2O/EtOH (7:3:2), 110 ºC, Mw, 19%-62%; For **9a**, $Pd(PPh_3)_4$, Na_2CO_3, dioxane, 40%; (**ii**) For **31**, aq.NaOH, THF; dimethylamine hydrochloride, HATU, DIPEA, DMF, 0 ºC-rt, 48 (2 steps); (**iii**) For **28-30**, CH_2Cl_2/TFA (4:1), rt, 80-90%; (**iv**) For **10h**, methanesulfonyl chloride, Et_3N, CH_2Cl_2, 0 ºC-rt, 69%; For **10i**, dimethylcarbamic chloride, Et_3N, CH_2Cl_2, 0 ºC-rt, 48%; For **10j**, 2-chloro-2-oxoethyl acetate, Et_3N, CH_2Cl_2, 0 ºC-rt, 48%; $LiOH{\cdot}H_2O$, MeOH/H_2O (3:2), rt, 58%.

Scheme 6. Synthesis of compounds 36a-l[a]

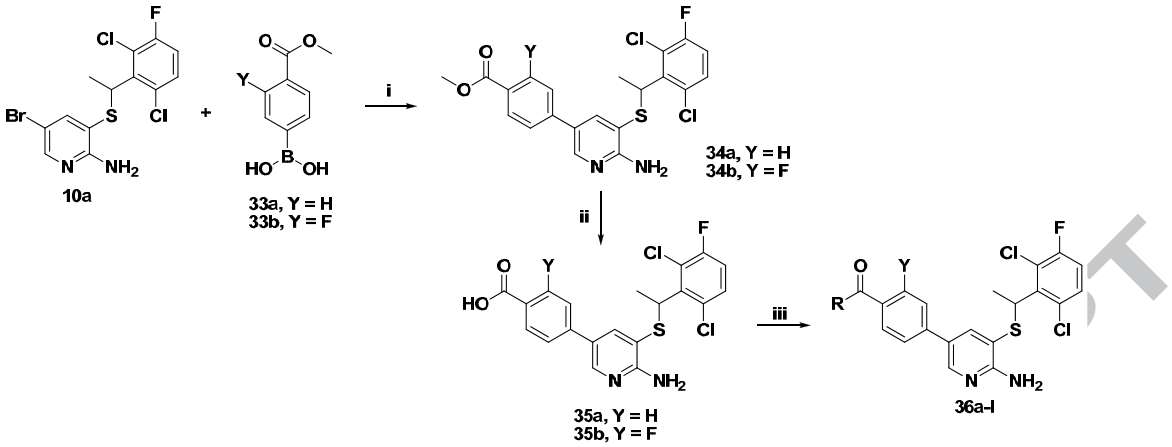

[a] Reagents and conditions: (**i**)$Pd(PPh_3)Cl_2$, Na_2CO_3, DME/H_2O(4:1), 80 ºC, 51% (**33b**); (**ii**)For **33a**, aq.NaOH, THF, 54% (2 steps); For **33b**, $LiOH{\cdot}H_2O$, MeOH/THF/H_2O (2:1:1), rt, 93%; (**iii**) For **36a-h**, HATU, DIPEA, DMF, 0 ºC-rt, 42-90%; For **36i-l**, EDCI, HOBT, Et_3N, CH_2Cl_2, 0 ºC-rt, 62-72%.

Scheme 7. Chiral synthesis of compounds (*R*)**-10b**[a]

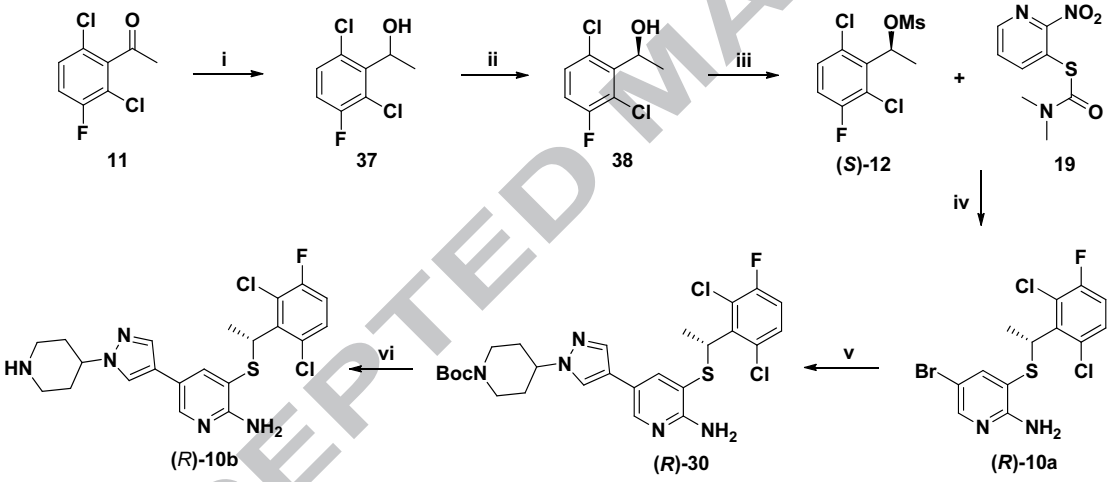

[a] Reagents and conditions: (**i**) $NaBH_4$, MeOH, rt; (**ii**) Boc-L-Pro, EDC, DMAP, $ClCH_2CH_2Cl$, -5 ºC, 58%; (**iii**) MsCl, Et_3N, 0 ºC-rt; (**iv**) KOH, MeOH/THF/H_2O (2:1:1), 0 ºC-rt; Fe/HCl, EtOH, reflux; Br_2, K_2CO_3, CH_2Cl_2, 0 ºC; (**v**) **25d**, $Pd(dppf)Cl_2$, Na_2CO_3, DMF/H_2O,80 ºC, 48%; (**vi**) TFA/CH_2Cl_2, rt.

Table 1. SAR about the linker X and pyrazole derivatives at the C-5 position

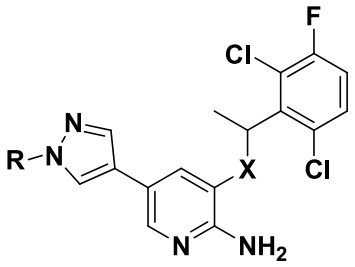

No.	R_1	X	IC_{50} (nM)	No.	R_1	X	IC_{50} (nM)
8b	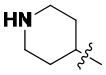		320.0 ± 80.0	**10e**	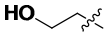	S	61.8 ± 4.1
8c			99.0 ± 20.0	**10f**		S	228.7 ± 43.2
8d			280.0 ± 40.0	**10g**	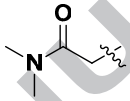	S	44.9 ± 4.7
9b	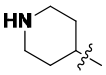		<u>19.4@10</u> μM	**10h**	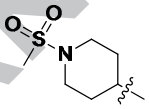	S	58.7 ± 1.1
10b	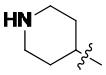	S	16.4 ± 1.5	**10i**	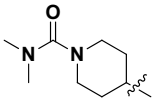	S	228.3 ± 32.2
10c		S	21.4 ± 5.7	**10j**	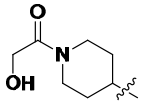	S	38.1 ± 4.5
10d		S	101.7 ± 19.9	**Crizotinib**	-	-	1.1 ± 0.1

Table 2. SAR about the aryl/heroaryl derivatives at the C-5 position

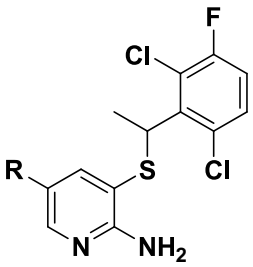

No.	R	IC_{50} (nM)	No.	R	IC_{50} (nM)
10k	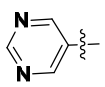	151.8 ± 22.6	**10n**	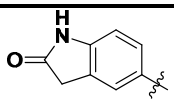	130.2 ± 0.1

10l	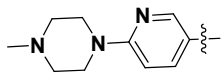	26.5 ± 0.0	**10o**	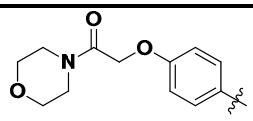	50.5 ± 2.5
10m	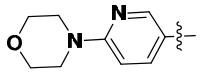	66.2 ± 15.7	**36a**	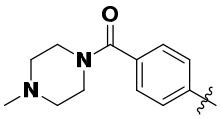	25.8 ± 5.2
Crizotinib	-	1.1 ± 0.1			

Table 3. SAR about the benzamides derivatives at the C-5 position

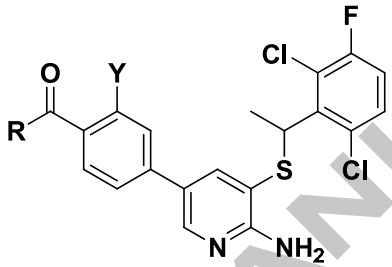

No.	R	Y	IC_{50} (nM）	No.	R	Y	IC_{50} (nM）
36a	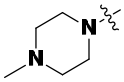	H	25.8 ± 5.2	**36g**	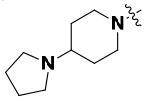	H	22.1 ± 0.3
36b	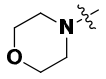	H	45.3 ± 3.8	**36h**	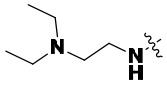	H	101.0 ± 12.4
36c		H	44.9 ± 8.7	**36i**	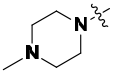	**F**	64.9 ± 9.3
36d	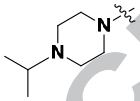	H	240.3 ± 66.9	**36j**	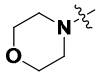	**F**	97.9 ± 6.7
36e	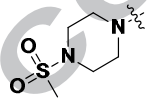	H	76.8 ± 7.9	**36k**		**F**	196.4 ± 12.5
36f	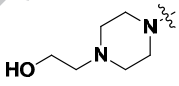	H	81.7 ± 21.9	**36l**	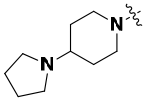	**F**	173.2 ± 14.1
Crizotinib	-	-	1.1 ± 0.1				

Table 4. Kinase Selectivity Profile of (*R*)-**10b**.

Kinase	Enzyme IC_{50} (nM)	Kinase	Enzyme IC_{50} (nM)
Met	7.7 ± 3.0	EGFR	＞1000
RON	336.4 ± 111.9	c-Kit	＞1000
Axl	446.5 ± 261.8	c-Src	＞1000
ALK	348.9 ± 153.1	Abl	＞1000
Tyro3	＞1000	EPH-A2	＞1000
PDGFRα	＞1000	EPH-B2	＞1000
PDGFRβ	＞1000	KDR	＞1000
FGFR1	＞1000	Flt-1	＞1000
RET	＞1000		

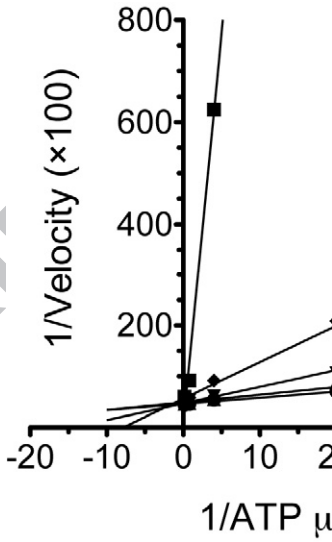

Figure 3. Lineweaver-Burk plot of ATP competition assay of (*R*)-**10b**.

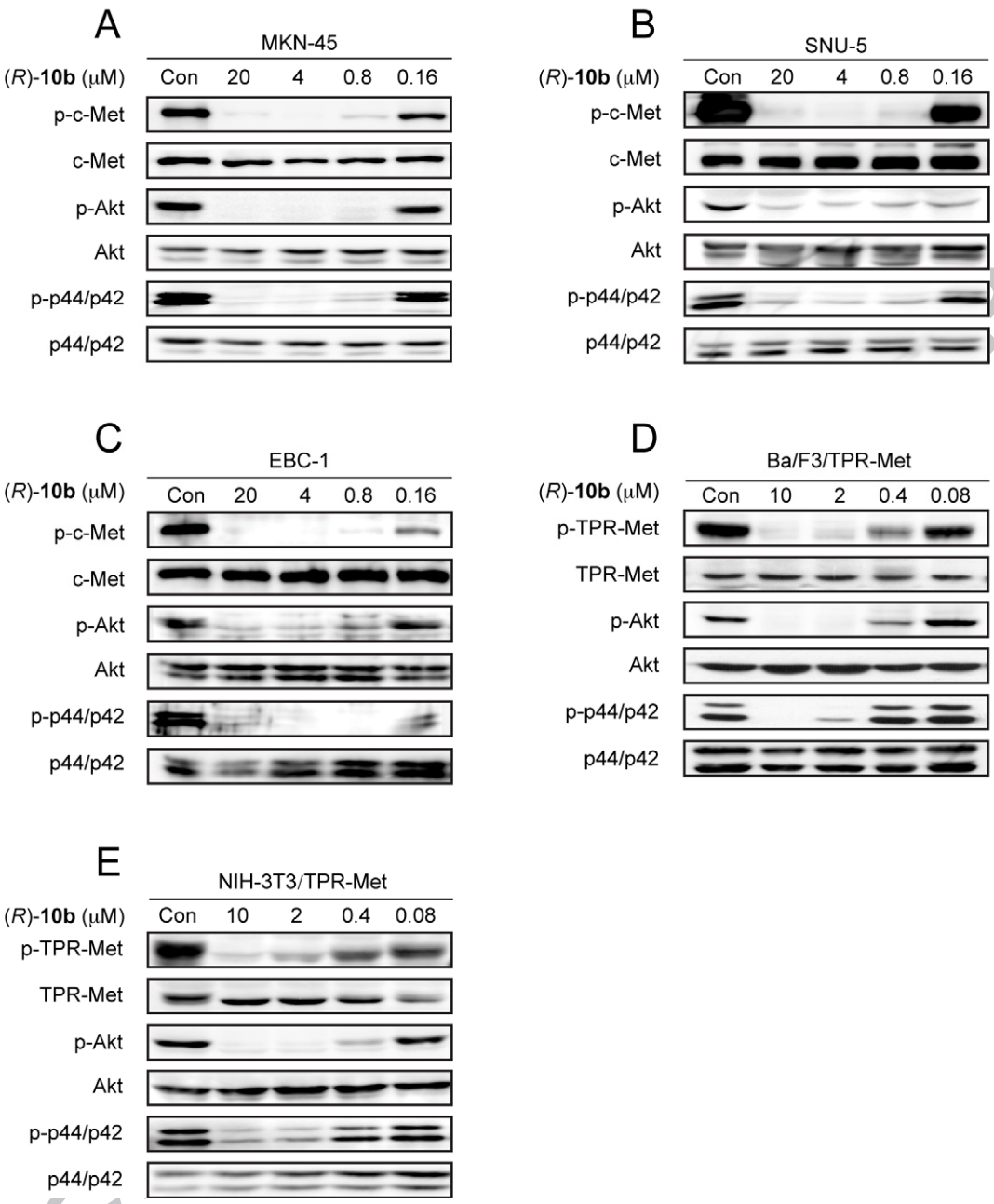

Figure 4. Dose-dependent inhibition of (*R*)-**10b** on c-Met phosphorylation and signal transduction pathways in MKN-45 (A), SNU-5 (B), EBC-1 (C), BaF3/TPR-Met (D) and NIH3T3-TPR-Met (E).

Table 5. Antiproliferative activity of (*R*)-**10b against human tumor cell lines.**

Cell line	(*R*)-**10b** IC_{50} (μM)	Crizotinib IC_{50} (μM)	Cell line	IC_{50} (μM)	Crizotinib IC_{50} (μM)
MKN-45	0.29 ± 0.05	0.013 ± 0.002	MCF-7	11.58 ± 5.51	9.58 ± 3.17
EBC-1	0.71 ± 0.16	0.023 ± 0.003	MDA-MB-231	12.10 ± 3.45	10.80 ± 2.30

SNU-5	0.19 ± 0.02	0.016 ± 0.003	SK-MEL-28	9.31 ± 2.16	10.97 ± 1.58
NCI-H441	15.51 ± 2.22	17.25 ± 2.66	SK-OV-3	12.73 ± 0.36	12.85 ± 0.29
NCI-H661	16.20 ± 1.82	11.47 ± 2.68	HCT-116	14.34 ± 3.41	14.82 ± 0.85

IC_{50}s were calculated as means ± SD (μM) from three separate experiments.

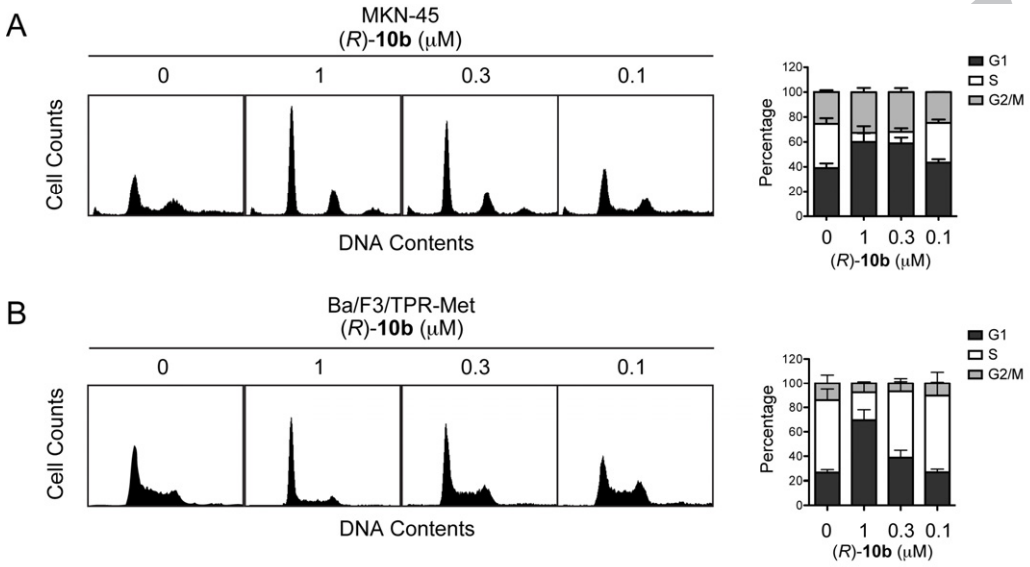

Figure 5. Inhibitory effects of (*R*)-**10b** on cell growth. Cell cycle arrest induced by (*R*)-**10b** in MKN-45 cell (A) and Ba/F3-TPR-Met cell (B).

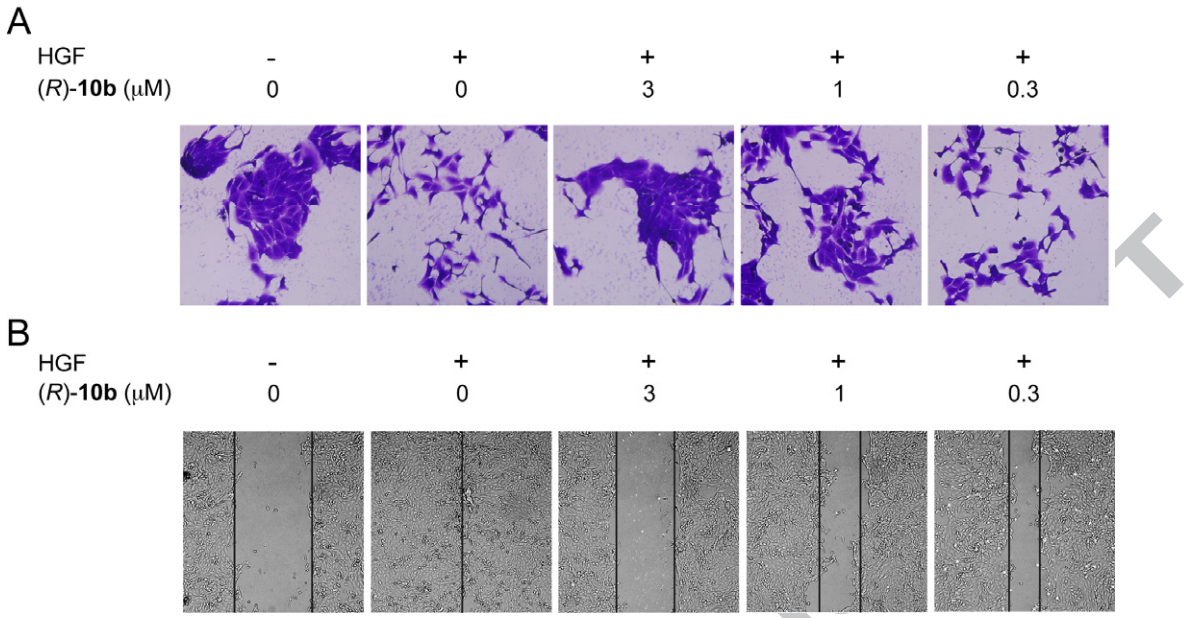

Figure 6. (*R*)-**10b** inhibits motility of MDCK cell on scattering assay (A) and wounding heal assay (B).

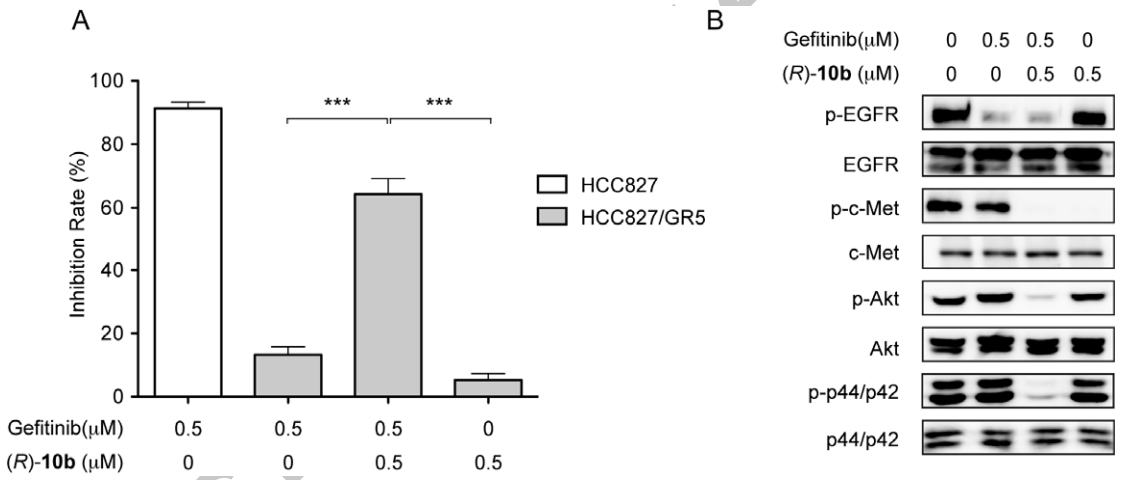

Figure 7. (*R*)-**10b** Overcomes gefitinib-Resistance. (*R*)-**10b** plus gefitinib inhibit gefitinib-resistant HCC827/GR5 cell proliferation (A), and downstream signal transduction pathways (B) in HCC827/GR5 cell line.

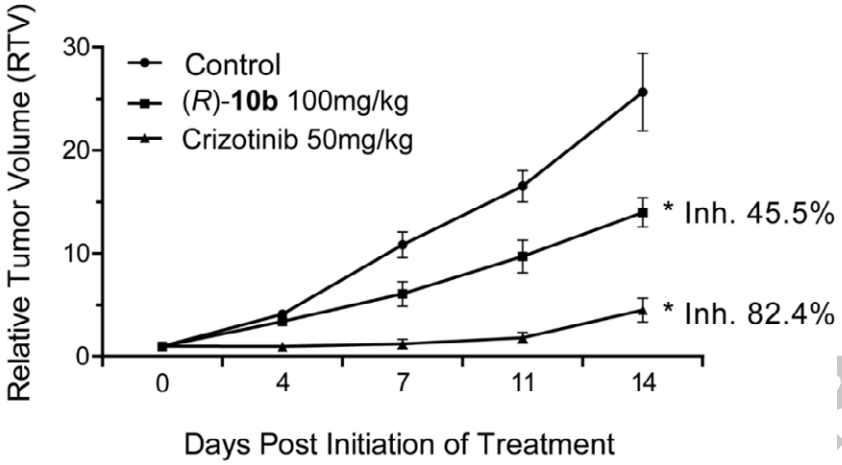

Figure 8. *In vivo* effect of (*R*)-**10b** on tumor growth inhibition in the NIH-3T3/TPR-Met xenograft model. (*R*)-**10b** and Crizotinib were administered by oral once daily for 2 weeks after the tumor volume reached 100 to 150 mm^3. Tumors were measured twice per week. Crizotinib was used as a reference compound. Results are expressed as mean ± standard error (n = 6 per group). Asterisk denotes $p < 0.05$ compared to treatment with control, determined with Student's *t*-test. Percent tumor growth inhibition values (Inh.) were measured on the final day of study for drug-treated compared with control mice and were calculated as $100\% \times \{1-[(Treated_{Day\ 14} - Treated_{Day\ 0})/ (Control_{Day\ 14} - Control_{Day0})]\}$.

Graphical Abstract

A series of 2-amino-*N*-benzylpyridine-3-carboxnamides, 2-amino-*N*-benzylpyridine-3-sulfonamides and 2-amino-3-benzylthiopyridines against c-Met were designed by means of bioisosteric replacement and docking analysis. Optimization of the 2-amino-3-benzylthiopyridine scaffold identified compound (*R*)-**10b** displaying c-Met inhibition with an IC_{50} up to 7.7 nM. In the cytotoxic evaluation, compound (*R*)-**10b** effectively inhibited the proliferation of c-Met addictive human cancer cell lines (IC_{50} from 0.19 - 0.71 μM) and c-Met activation-mediated cell metastasis. Of note, (*R*)-**10b** could overcome c-Met-activation mediated gefitinib-resistance. (*R*)-**10b** could inhibit moderate inhibition of tumor growth (45%) in NIH-3T3/TPR-Met xenograft model probably due to its high clearance and low bioavailability.

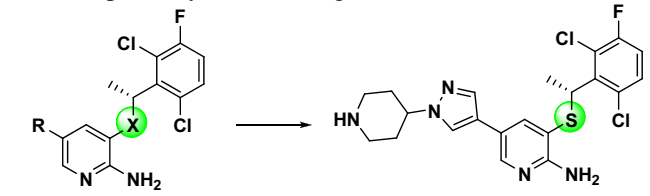

c-Met IC_{50} = 7.7 nM, SNU: IC_{50} = 0.19 μM
MKN45: IC_{50} = 0.29 μM, EBC-1: IC_{50} = 0.71 μM
effectively overcome c-Met-activation mediated gefitinib-resistance